ELSEVIER

Contents lists available at ScienceDirect

Geomorphology

journal homepage: www.journals.elsevier.com/geomorphology





Quaternary tectonic and climatic forcing on the spatio-temporal evolution of the Meuse fluvial terrace staircase

Ewerton da Silva Guimarães ^{a,b,*}, Freek S. Busschers ^{b,**}, Cornelis Kasse ^a, Tom Van Haren ^c, Armin Menkovic ^b, Ronald T. Van Balen ^{a,b}

- ^a Department of Earth Sciences, Vrije Universiteit Amsterdam, De Boelelaan 1085, 1081 HV Amsterdam, the Netherlands
- ^b TNO Geological Survey of the Netherlands, Princetonlaan 6, 3584 CB Utrecht, the Netherlands
- ^c VITO Flemish Institute for Technological Research, Boeretang 200, BE-2400 Mol, Belgium

ARTICLE INFO

Keywords:
Mid-Pleistocene Transition
Terrace lithology
River gradients
Uplift
East Meuse valley
Ardennes

ABSTRACT

The Quaternary is characterized by pronounced alterations between cold and warm climatic states, with the Mid-Pleistocene Transition marking a strong increase in the intensity of cold-climate conditions. River systems are sensitive to environmental perturbation (e.g., climate, tectonics, base level) and are expected to respond to such profound changes. This study uses a combination of terrace mapping and analysis of a dense borehole database to investigate the Meuse terrace staircase (and its deposits), and gain insight on how it reflects climatic and tectonic perturbations during the Quaternary. The lower reaches of the Meuse river, which has both its main water and sediment source in the Ardennes displays a well-developed terrace staircase that was sculpted mainly throughout the Quaternary. The staircase is located near the cities of Maastricht (southern Netherlands) and Liège (northwestern Belgium). About 30 terrace levels reflect signals of environmental perturbations in the lithological composition, gradients, thicknesses, and spatial distribution. The terraces are organized in groups, based on their morphological position, from old to young; these are the East Meuse terrace group and West Meuse High-, Middle- and Low terrace groups. Our findings show a consistent increase in the gravel content from older to younger terraces. The sandier composition of the deposits of the oldest terraces (Early Pleistocene) is closely related to the supply of the Miocene-Pliocene weathered material from the Ardennes. Younger terraces (Middle and Late Pleistocene) are much richer in gravel, evidencing sediment input from fresh or partially weathered bedrock. These changes point to a downstream migration of the gravel front throughout the Quaternary. The mean thickness of the terrace groups shows a slight increase, even though the same trend is not clear when each terrace is analyzed on an individual basis. The anomalous thickness of the Caberg 1 terrace suggests increased sediment input during the cold climatic conditions of the Elsterian (MIS 12), the first Quaternary glacial during which an ice sheet extended into the northern Netherlands. Reconstruction of terrace gradients reveals that older East Meuse terraces show a (reversed) gradient opposite to reconstructed palaeo flow directions, which is attributed to a combination of low gradients during terrace formation and footwall back-tilting of the Feldbiss Fault Zone. In our analysis we do not see clear evidence for the imprint of the Mid-Pleistocene Transition, which suggests that due to its gradual nature, its signal is either buffered or assimilated by the overall climatic signal of the Quaternary. This study offers a first complete temporal analysis of the Meuse terrace staircase, providing an important basis for better understanding the effects of Quaternary climatic change and tectonics, and their resulting effects in other river systems worldwide.

E-mail addresses: e.dasilvaguimaraes@vu.nl (E. da Silva Guimarães), freek.busschers@tno.nl (F.S. Busschers).

^{*} Correspondence to: E. da Silva Guimarães, Department of Earth Sciences, Vrije Universiteit Amsterdam, De Boelelaan 1085, 1081 HV Amsterdam, the Netherlands.

^{**} Corresponding author.

1. Introduction

The Quaternary is marked by strong climatic oscillations that left major imprints on both marine and continental environments. Compared to the Pliocene, Quaternary climate oscillations were generally of higher amplitude with deeper glacial minima (Lisiecki and Raymo, 2005; Head and Gibbard, 2015; Ehlers et al., 2018). During several glacial minima, large ice sheets developed, especially in the Northern Hemisphere (Ehlers et al., 2018; Rea et al., 2018), mirrored in global sea-level cycles with minima between 100 and 140 m below, and maxima within 10 m above the present sea-level (Anderson et al., 2013; Spratt and Lisiecki, 2016). The Quaternary climate is characterized by a significant and pivotal period between ca. 1.25 and ca. 0.65 Ma (Ruddiman et al., 1986; Clark et al., 2006), known as the Mid-Pleistocene Transition (MPT). It reflects a transitional phase between a period with primarily symmetric 41-kyr cycles during the Early Pleistocene to a time interval of strongly asymmetric 100-kyr cycles, with much larger climatic amplitudes and substantial intensification of cold-climate conditions, during the Middle and Late Pleistocene (Ruddiman et al., 1986; Lisiecki and Raymo, 2007). As orbital parameters did not change (Pisias and Moore, 1981; Clark et al., 2006), the MPT is regarded as a product of internal mechanisms of Earth's climate system (Maslin and Ridgwell, 2005). Although the exact causes for this significant change are still debated, and different hypotheses are proposed, a combination of CO₂ decrease, and progressive glacial regolith erosion is regarded critical (Berends et al., 2021).

For instance, the gradual (glacial) erosion of regolith in high latitudes of the Northern Hemisphere increased basal friction between the ice sheets and bedrock, and thus allowed the build-up of increasingly thicker ice masses that withstood melting processes over the 41 kyr cycles (Clark and Pollard, 1998; Clark et al., 2006; Sosdian and Rosenthal, 2009; Yehudai et al., 2021). The formation of these extensive ice masses may be attributed to a prolonged cooling trend accompanied by increase in the climate amplitude during the Quaternary, driven by declining sea surface temperatures and changes in oceanic circulation (e.g., Herbert et al., 2010; Lawrence et al., 2010; McClymont et al., 2013). In turn, this cooling trend is often linked to a reduction in atmospheric CO2 levels, as CO2 solubility increases with decreasing sea surface temperatures (Millero, 1995; Clark et al., 2006). Furthermore, progressive regolith erosion resulted in the production of substantial amounts of glaciogenic dust. The influx of this dust into the oceans significantly influenced productivity by fertilizing the waters, leading to increased levels of phytoplankton and their subsequent uptake of CO₂ for metabolic purposes (Martin et al., 1990; Martínez-García et al., 2014; Müller et al., 2018). Also linked to long-term cooling is the hypothesis of Arctic sea-ice growth (Gildor and Tziperman, 2001) and the expansion of the East (Raymo et al., 2006) and the West Antarctic ice sheet (Lawrence et al., 2010). A thorough review on the MPT and the Quaternary climatic change is given by Zachos et al. (2001), Maslin and Ridgwell (2005), Head and Gibbard (2015), and Berends et al. (2021).

Despite the clear identification of the Quaternary climatic changes in the marine sedimentary records, the same is not true for the imprint of these changes in the terrestrial realm (Bridgland and Westaway, 2008; Gibbard and Lewin, 2009; Head and Gibbard, 2015), making, for example, coupling of terrestrial sources to (dominantly marine) sinks challenging at best. Fluvial terrace staircases are important geomorphic and stratigraphic archives of the long- and short-term temporal evolution of fluvial landscapes and therefore can bear critical records of terrestrial response to the Quaternary climate changes (Van Balen et al., 2000; Schaller et al., 2004; Fuller et al., 2009; Vandermaelen et al., 2022).

In general, a fluvial terrace is a former river floodplain that is now at an elevated position (Bull, 1991; Pazzaglia, 2013). It can occur in a wide range of physiographic settings (Pazzaglia, 2013), from lowlands (e.g., Van Balen et al., 2000; Van den Berg and Van Hoof, 2001; Boenigk and Frechen, 2006) to mountain ranges (e.g., Tofelde et al., 2017). A fluvial

terrace forms when a river incises, abandons its floodplain, and forms a new floodplain at a lower level. A terrace staircase is composed of terraces at different elevations. They form due to an alternation of downcutting and aggradation or a reduced downcutting rate during long-term incision (Vandenberghe, 2015). In many cases, the long-term incision is a result of tectonic uplift, whereas terrace formation is climate controlled (e.g., Maddy et al., 2001). Alternative triggers of terrace formation are, for example, faulting (Su et al., 2024), and riverdamming events, such as lava-flows and slope collapse, and associated base-level changes (e.g., Maddy et al., 2007; Tost et al., 2015).

The relation between climate change and terrace formation can be complicated. Vandenberghe (2008, 2015) and Bridgland and Westaway (2008) propose scenarios for climate-driven terrace formation of lowland rivers based on well-dated late Pleistocene fluvial sequences in north-west Europe. Aggradation occurs during cold periods with limited vegetation cover and high sediment supply. Vertical incision occurs at the cold-warm transition, due to the action of meandering channels (low width-depth ratio), thus abandoning cold-period deposits of a previous braided system and forming a terrace. Stability prevails during the warm period. During the subsequent warm-cold transition, a second and more dominant lateral erosion phase by braided channels (high width-depth ratio) occurs (Vandenberghe, 2008). This erosion phase is laterally pronounced and (partly) removes previous warm-period deposits, and therefore the fluvial record is only partly preserved. As a result, coldperiod deposits dominate the terrace deposits, as evidenced by coldclimatic indicators such as fluvial style, periglacial deformations, and ice-rafted debris. Thus, terrace deposition ages can be tentatively estimated based on correlations with the well constrained marine isotope stages (Lisiecki and Raymo, 2005); several examples are presented in Bridgland and Westaway (2008) and Van den Berg and Van Hoof (2001). Additional age constraints are provided by dating methods like paleomagnetic dating, cosmogenic nuclide dating, and luminescence dating (cf., Van Balen et al., 2000; Rixhon et al., 2017).

Based on the Quaternary chronological framework, previous studies on terraces of NW European rivers, particularly the Meuse and the Rhine, suggest that Quaternary climate change, especially the MPT, drove a general increase in sediment caliber of terrace deposits. This increase was accompanied by higher gravel content and incision rates (e. g., Van Balen et al., 2000; Schaller et al., 2004; Boenigk and Frechen, 2006; Bridgland and Westaway, 2008; Gibbard and Lewin, 2009). The increased incision rates are expressed by a slope break bounding an inner valley with terrace remnants of smaller widths and larger incisional steps compared to the higher terraces. Examples thereof are the Middle and Lower Rhine (Van Balen et al., 2000; Meyer and Stets, 2002; Boenigk and Frechen, 2006), the Vltava (Tyráček et al., 2004), the Dniester (Matoshko et al., 2004), the Thames (Bridgland, 1995, 2006; Gibbard and Lewin, 2003) and the Meuse (Van den Berg, 1996; Van Balen et al., 2000). However, the MPT is a gradual transition, whereas the inner valley formation in the Meuse and Rhine valleys reflects an abrupt change. For the Rhine and Meuse systems, the increased incision rates have therefore also been explained by increased tectonic uplift (Van Balen et al., 2000; Rixhon et al., 2011; Demoulin et al., 2012).

Despite the general observations that were previously made for these systems, quantitative data on the imprint of Quaternary climatic changes on fluvial terrace staircases are not available so far. In this study, we address the Meuse terrace staircase in the southern Netherlands and adjoining areas in Belgium and Germany. We hereby quantify changes in gravel-sand ratio, terrace deposit thickness, gradient, and incision in order to make a sequential order of events of the Meuse terrace staircase evolution, allowing comparison for different time periods and assess differences through time. Our analysis is based on the terrace formation model proposed by Vandenberghe (2008, 2015) and the terrace age model proposed by Van den Berg (1996) and Van den Berg and Van Hoof (2001). Our methods rely on an updated Meuse terrace map using new borehole and morphological data combined with a compilation of published maps and a vast database of

boreholes from the Netherlands and Belgium. This map supports the characterization of composition and geometry of the Meuse terraces, which are analyzed individually (per terrace level) and in groups. This work presents a first full analysis of the Meuse terrace staircase through time, providing an important basis for better understanding the effects of Quaternary climatic change and tectonics, and their resulting effects in other river systems worldwide.

2. Study area

2.1. Physiographic and tectonic setting

The Meuse is a ca. 900 km long rainfed river system with a current catchment area of approximately $33,000\,\mathrm{km}^2$. It crosses three large-scale morphotectonic domains (Fig. 1a). The headwaters are located on the northeastern margin of the Paris Basin (mostly Jurassic and Cretaceous limestones), close to the Vosges mountains. Subsequently, it crosses the western part of the uplifting Ardennes massif in Belgium (mostly Paleozoic quartzites, sandstones, shales and carbonates) before reaching the Cretaceous and Tertiary sediments of the southern part of the Netherlands. The river then crosses the active Roer Valley Rift System (RVRS) before joining the Rhine river in the central part of the Netherlands and debouching into the North Sea.

The RVRS is an active extensional structure located in the southeastern part of the Netherlands and adjoining areas in Germany and Belgium. It is part of the Lower Rhine Embayment (LRE), which in turn is included in the West European rift system (Ziegler, 1992). From south to north the RVRS comprises the uplifting Campine and South Limburg Blocks, the subsiding Roer Valley Graben (RVG; Fig. 1b), the uplifting Peel Block, and the Venlo Graben (see Van Balen et al., 2005). The Feldbiss Fault Zone (FFZ) bounds the RVG in the south, whereas the Peel Boundary Fault Zone (PBFZ) marks its northern boundary. The RVRS has a long tectonic history that comprises several Mesozoic and Cenozoic extension and inversion phases. The most recent extensional phase started at the Oligocene–Miocene transition and is still ongoing (Geluk et al., 1994; Van Balen et al., 2005).

Upstream, the Ardennes is the western part of the Rhenish massif, which originated during the Variscan orogeny. It experienced moderate late Cenozoic uplift continuing up to Present-day, as a response to Alpine compression (Ziegler and Dèzes, 2007) and, during the Middle Pleistocene, to mantle upwelling (Van Balen et al., 2000; Meyer and Stets, 2002; Ziegler and Dèzes, 2007; Demoulin and Hallot, 2009). The upheaval of the Ardennes and Rhenish massifs by Alpine compression and plume uplift is evidenced by Mesozoic to Early Cenozoic (up to Miocene) planation surfaces, which are now at an elevated position, and are deformed (Demoulin et al., 2018). An acceleration of the uplift rates in the Rhenish and Ardennes massifs during the Quaternary was identified by unraveling the terrace staircases of the Meuse and Rhine rivers and their tributaries. This acceleration occurred at the Plio-Pleistocene transition and again in the Middle Pleistocene (plume uplift), reaching

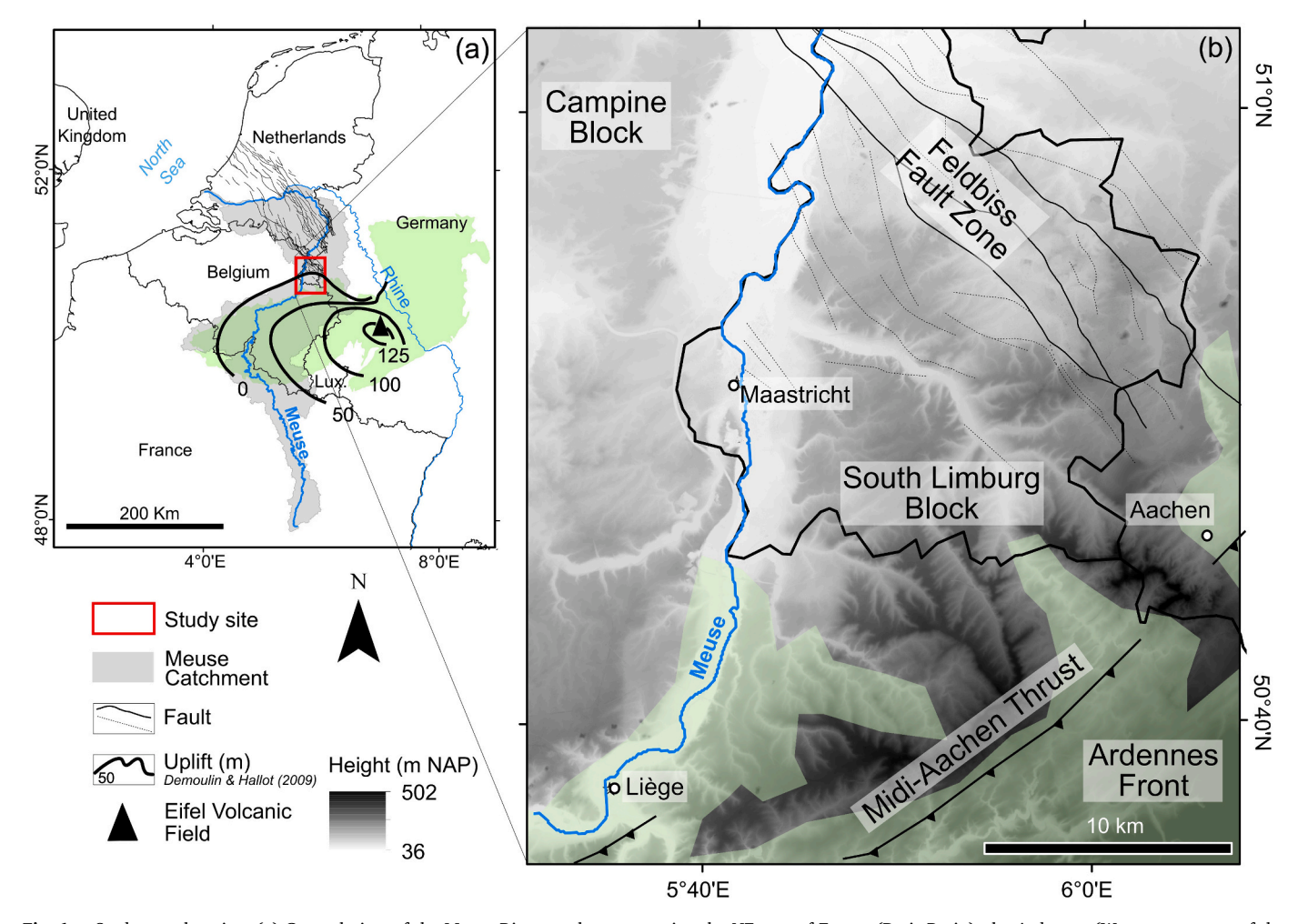


Fig. 1.: Study area location. (a) General view of the Meuse River catchment crossing the NE part of France (Paris Basin), the Ardennes (Western segment of the Rhenish Massif), and the Roer Valley Rift System (RVRS). Bold lines represent the estimated amount of uplift in meters since the beginning of the Middle Pleistocene (Demoulin and Hallot, 2009; see also Kreemer et al., 2020; Meyer and Stets, 1998; Van Balen et al., 2000); (b) The study area is located immediately downstream of the Ardennes and upstream of the Feldbiss Fault Zone, the southern border of the Roer Valley Graben.

values of up to ca. 500 mm/ka in the period around 0.75–0.4 Ma (Van den Berg, 1996; Van Balen et al., 2000; Boenigk and Frechen, 2006). These changes in uplift rates are inferred from fluvial valley morphology. In the upper part of these valleys (Pliocene-Early Pleistocene in age) the terraces are wide and have small incisional steps, whereas in the lower inner-valleys (Middle- and Late-Pleistocene) they are narrow and have large steps (Van Balen et al., 2000; Boenigk and Frechen, 2006; Rixhon et al., 2011). According to Demoulin and Hallot (2009), this last pulse of uplift caused the Ardennes to rise ca. 100–200 m. Traditionally, the terraces of the wide valley system are called Main or High terraces, whereas those of the inner valley are called Middle and

Lower terraces.

The study area is located in the area of uplift situated on the northern part of the Ardennes and the southern shoulder of the RVRS. It is bounded in the north by the FFZ, and it comprises the South Limburg and Campine tectonic blocks (Fig. 1b). The uplift has caused long-term incision and, in combination with climate change, the formation of a terrace staircase by the Meuse river (Van den Berg, 1996; Van Balen et al., 2000; Rixhon and Demoulin, 2018). We focus on this uplifting area to avoid the effect of terrace stacking, which occurs in the subsidence-controlled areas north of the FFZ, in the central RVG of the RVRS.

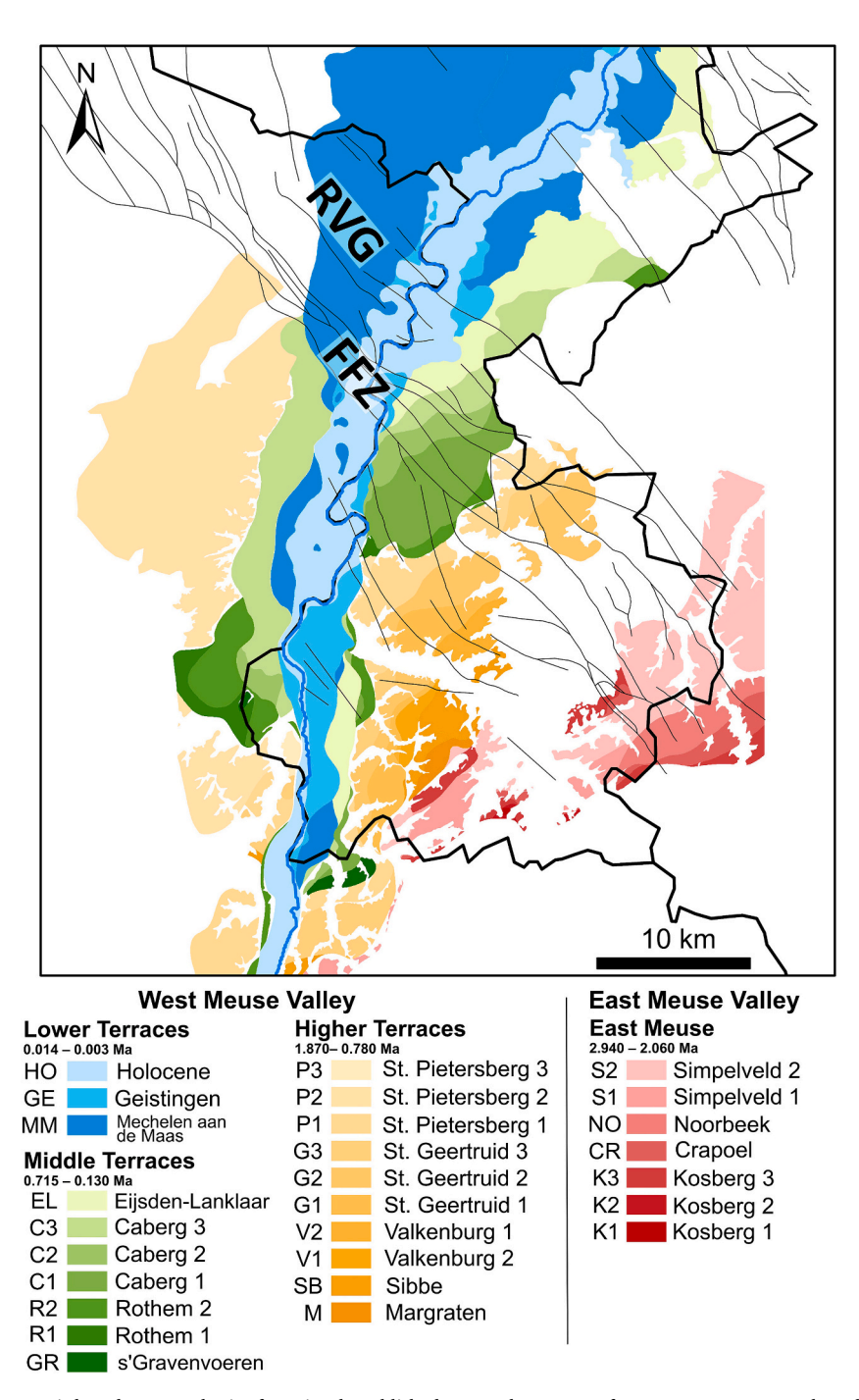


Fig. 2. Meuse terrace map. The map is based on a synthesis of previously published maps. The extents of some terrace remnants have been updated based on a novel high resolution LiDAR DEM. The terrace levels labelling as well as the age span of terrace groups (see Table 1) are after Van den Berg (1996), and Van den Berg and Van Hoof (2001). The terraces are separated in four major groups: from older to younger East Meuse Terraces, which belongs to the currently abandoned East Meuse Valley; Higher, Middle and Lower Terraces, which belong to the currently active West Meuse Valley. RVG: Roer Valley Graben; FFZ: Feldbiss Fault Zone.

2.2. Morphostructural setting and terrace development

During the Late Pliocene the Meuse occupied the East Meuse valley, a currently abandoned valley located in the south-eastern most area of the Netherlands and adjoining area in Germany (Fig. 2). The Meuse confluenced with the Rhine near Cologne. From there, the Rhine-Meuse system continued to flow into the Roer Valley Graben, dictated by the tectonic structure of the RVRS.

During the Early Pleistocene period, the Meuse River shifted from its previous route in the East Meuse valley to begin sculpting the West Meuse valley (Fig. 2). The exact mechanism responsible for this course change remains uncertain, but it is likely associated with factors such as the Cretaceous limestone subsurface, triggering karstic processes (e.g., Losson and Quinif, 2001) and the effects of tectonic activity on gradients (the previous course of the Meuse in the East Meuse valley was oriented according to changing tectonic motions in the area).

During the early Middle Pleistocene (Marine Isotope Stage 16), the Rhine permanently abandoned the RVG (Boenigk, 1978; Zagwijn, 1985; Boenigk and Frechen, 2006). Finally, also the Meuse left the RVG during the late Middle Pleistocene (ca. 250 ka; MIS 8) and began to flow across the Peel Block. From the late Saalian (150 ka; MIS 6), the Meuse formed terraces at its current location on the Peel Block. Up to the Weichselian and Holocene, whereas in the study area the terraces span the whole of the Quaternary.

About thirty different terrace levels were discriminated in the study area (Fig. 2; see also Felder and Bosch, 1989; Van den Berg, 1989). The number of terraces decreases upstream, likely as a result of the decreasing degree of preservation of terrace deposits. For example, around ten levels were identified where the Meuse crosses the Ardennes, upstream of the study area (Macar, 1938, 1954; Juvigné and Renard, 1992; Pissart et al., 1997; Van Balen et al., 2000). The larger number of terrace levels in the study area is due to its favorable position between the RVG (subsidence controlled) and Ardennes (uplift controlled; Veldkamp and Van Dijke, 2000).

The state of preservation of the terraces varies. In general, the older terraces are less preserved due to post-formation weathering and erosion (Van den Berg, 1996). The thickness of the terrace remnants varies considerably, ranging from a few meters up to 25 m (Van den Berg and Van Hoof, 2001). They are mostly composed of gravel (mostly Paleozoic quartz, quartzite and sandstone, and Cretaceous flint) and coarse sand, with rare occurrences of clay deposits and paleosols (Macar, 1938, 1954; Breuren, 1945; Van Straaten, 1946; Zonneveld, 1949; Felder and Bosch, 1989; Van Kolfschoten et al., 1993; Van den Berg and Van Hoof, 2001). The gravel and sand deposits contain characteristics of cold-climate environments such as ice-wedge casts, cryoturbations, and large, msize boulders, the latter probably transported by ice-rafting (Collard et al., 2012; Houbrechts et al., 2018). Alternatively, De Brue et al. (2015) propose purely hydraulic transport modes for these large boulders, which rely on lowered hydraulic transport thresholds and catastrophic floods caused by ice jams and dam collapse. The predominance of coarse bedload in a relatively wide area of sheet-like morphology indicates braided-style channel deposits (Van den Berg, 1996).

The age control of the terrace deposits is based on a variety of age-dating methods. In general, younger terrace levels were dated by numerical dating methods (Huxtable, 1993; Van Kolfschoten et al., 1993; Schaller et al., 2004; Houtgast et al., 2005; Meijer and Cleveringa, 2009; Rixhon et al., 2011; Woolderink et al., 2019; Van Balen et al., 2021); older levels have been dated indirectly by correlation with the marine isotopic stage record (assuming deposition during cold stages), biostratigraphy, paleomagnetic data, and regional correlations (Felder and Bosch, 1989; Van den Berg, 1996; Pissart et al., 1997; Van Balen et al., 2000; Westaway, 2001; Houtgast et al., 2002). Table 1 shows an overview of the age constraints.

2.3. The Meuse terraces and their Quaternary climate archive

The Paleozoic rocks of the Ardennes are the most important source of sediment composing the Meuse terrace deposits (Van den Berg and Van Hoof, 2001). Its pre-Quaternary morphologic history is marked by intense weathering events under (sub) tropical conditions during the Early Miocene, and marine transgressions during the Oligocene-Miocene (Demoulin, 1995; Demoulin et al., 2018). Thus, most of the sediment composing the older Meuse terraces is a product of the quartz-enriched weathering overburden of the Ardennes (Tesch, 1941), which started to be eroded following the climate changes in the Late Pliocene and Quaternary. An important characteristic of the Meuse terraces is the decrease in quartz content (Van Straaten, 1946) and stable heavy mineral content from older to younger terraces (Zonneveld, 1949; Bustamante-Santa Cruz, 1973; Krook, 1993; Westerhoff et al., 2008). Thus, the East Meuse terraces, especially the Kosberg levels, are rich in quartz and stable heavy minerals, resembling the composition of Pliocene deposits of the RVRS (Kieseloolite Formation; see Boenigk and Frechen, 2006; Westerhoff et al., 2008). On the other hand, younger levels gradually become enriched with fresh rock components (Paleozoic quartzites and sandstones) and are impoverished in quartz and stable heavy mineral contents. These observations testify to increasing incision and periglacial weathering processes throughout the Quaternary (Van den Berg, 1996). Similar observations are also reported for the Middle and Lower Rhine (Boenigk and Frechen, 2006; Kemna, 2008; Westerhoff et al., 2008).

3. Methods

3.1. Borehole data

In the Dutch area, we extracted data from the DINO borehole database, the national Dutch subsurface database, which is operated by the TNO - Geological Survey of the Netherlands (extraction date 08-04-2022; www.dinoloket.nl; Van der Meulen et al., 2013). We only extracted those borehole logs that contained lithostratigraphically coded information referred to as Beegden Formation, which represents sediments deposited by the Pleistocene Meuse in the Netherlands.

For the Belgian area, we extracted data from the Flanders Online Soil and Subsoil Database, which is operated by the government of Flanders (www.dov.vlaanderen.be). These borehole data were lithologically coded, stratigraphically (re)interpreted, and organized in a separate database by Van Haren et al. (2016a, 2016b). This borehole data was converted into Dutch standard coordinate system (RD New) and elevation reference (NAP), and all lithological and admixture attributes were transformed into SBB 5.1 format (Bosch, 2000) as used by TNO Geological Survey of the Netherlands. We only used information from those borehole intervals that were assigned the stratigraphic codes 'Rafz', 'Maasgroep' and 'Beegden zg, k1 & k2' (see Section 4.3 in Van Haren et al., 2016b). As the lower part of these intervals locally contains mostly finer-grained sediments that occur below the base of the Meuse terraces in this area, we only used those intervals that contained a gravelly base, thus ensuring stratigraphic synchroneity between the Dutch and Belgian datasets.

The so-called Winterslag Sands (Gullentops et al., 2001; Van Haren et al., 2016b; Beerten et al., 2018) were not included in this study. They represent an older (final Early Pleistocene) Meuse sand deposit that underlie the Meuse terrace gravel accumulation on the Campine plateau (Zutendaal Gravels; see Fig. 4 in Van Haren et al., 2016b). Furthermore, borehole intervals interpreted as 'Maasgroep' but belonging to the Lommel or Bocholt Members were excluded due to mixing with Rhine sediments (cf. Gullentops et al., 2001; Beerten et al., 2018).

The synchronized Belgian and Dutch borehole data sets were combined into one database. Subsequently, borehole logs with poor or no description, with lithological interval(s) thicker than 10 m and/or with incorrect location coordinates, were excluded from the dataset. From

Table 1

Overview of the age control for the Lower Meuse Terraces. This table highlights the most important age-dates for this study. More age-dates are available in the literature for the Weichselian and Holocene levels.

	Terrace level	Estimated age (ka) — indirect methods						Estimated age (ka) — direct methods							
Terrace group		Van den Berg, 1996	Felder and Bosch, 1989	Van Balen et al., 2000	Houtgast et al., 2002	Westaway, 2001	Pissart et al., 1997	Rixhon et al., 2011	Rixhon and Demoulin, 2018	Huxtable, 1993	Van Kolfschoten et al., 1993	Meijer and Cleveringa, 2009	Schaller et al., 2004	Houtgast et al., 2005	Van Balen et al. (2021)
Lower terraces	Holocene floodplain	3													
	Geistingen	11	13		11										
	Mechelen a/ d Maas	14		14	14	14									
Middle terraces	Eisden Lanklaar	130		130	130	130									
	Caberg 3	245	250	250	250	245	245			250 ± 20^3	220 ± 40^4	$340-300^5$		$> 89 \pm 9^{6}$	
	Caberg 2	330			330	330									343 (-45, +56) ⁷
	Caberg 1	420			420	420									+30)
	Rothem 2	510		430	530	470	330								
	Rothem 1	620	520		600	510	420								
	Gravenvoeren	715		650	650	620	510								
Higher	Pietersberg 3	780			710	700			625 ²						
terraces	Pietersberg 2	870			750	780	620	$725 \pm \\120^1$					1060 ± 260^1		
	Pietersberg 1	955	700	720	780	870	715								
	Geertruid 3	1030		850	850	1030									
	Geertruid 2	1090			980	1090	870						1720 ± 220^1		
	Geertruid 1	1280	1050	1110	1100	1280	1100						1690 ± 500^1		
	Valkenburg 2	1500				1420	1200								
	Valkenburg 1	1570	1300			1460	1280								
	Sibbe 2	1690				1570	1420								
	Sibbe 1	1740	1410/1800	1500		1650	1420								
	Margraten	1870				1740	1570								
East Meuse	Simpelveld 2	2060				1820	1820								
terraces	Simpelveld 1	2140													
	Noorbeek	2440					1930								
	Crapoel	2600					2030								
	Kosberg 3	2690													
	Kosberg 2	2810													
	Kosberg 1	2940													

Cosmogenic radionuclide.
 Reinterpretation of previous results.
 Thermo-luminescence.

⁴ Electron spin resonance.

⁵ Amino-acids.

⁶ Optical stimulated luminescence.

⁷ Infra-red stimulated luminescence.

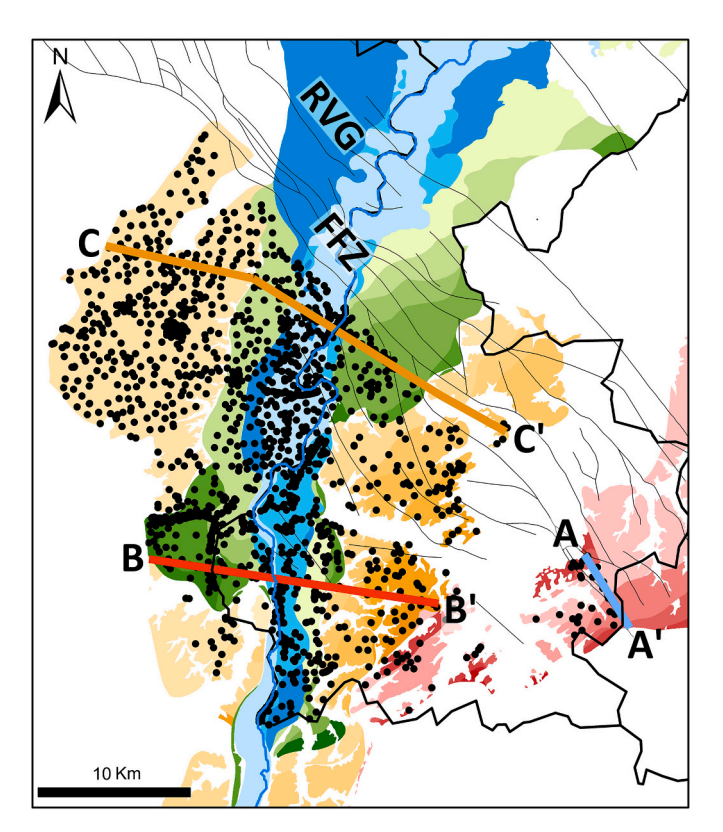


Fig. 3.: Overview of the borehole database used in this study and location of cross-section A–A′, B–B′ and C–C′ (Fig. 5). A complete legend for color coded terraces is displayed in Fig. 2. RVG: Roer Valley Graben; FFZ: Feldbiss Fault Zone.

this resulting dataset, we then excluded those boreholes that were positioned too close to the Roer Valley Graben (hereby using a 1-km radius buffer zone along the Feldbiss Faultzone), in order to exclude the impact of subsidence-driven sediment stacking on our results (Fig. 3).

All steps described above were performed using a combination of Python and (Python-steered) ArcMap 10.6 commands and resulted in a final database of 2777 boreholes that we used for subsequent investigation (Fig. 3).

3.2. Terrace map

The terrace map was made by compiling previously published terrace maps (Fig. 2; Macar, 1938; Felder and Bosch, 1989; Van den Berg, 1989), and updating them with new information from (i) newly coded borehole data, (ii) a distribution map of the Beegden Formation (TNO-GDN; www.dinoloket.nl) and (iii) morphologic analyzes of relatively recent high resolution Digital Elevation Models based on LiDAR (AHN, version 2; www.ahn.nl). The terrace map covers the southern Netherlands and adjoining areas in northeastern Belgium and western Germany. Felder and Bosch (1989) mapped the terraces based on geomorphology and borehole data, using the terrace base elevation to delineate the terrace boundaries. Van den Berg (1989) used the terrace top elevation for tracing terrace boundaries, arguing that these vary considerably less than the base elevations.

The Felder and Bosch (1989) map was used as a template for the updated map because it covers a larger part of the area of interest south of the Feldbiss Fault Zone, especially over the East Meuse terraces. Besides, despite its coverage focusing on the Dutch area, the map coverage also includes Belgian and German adjoining areas containing Meuse terraces. It was then supplemented by the map from Macar (1938), who identified patches of terraces between Liège (Belgium) and Maastricht

(Netherlands), and overlapping terrace remnants were better delineated. Next, the mapping results from Van den Berg (1989) were then added for additional terraces.

Afterward, to confirm or modify the extent of each terrace, the borehole data were used in combination with the Beegden Formation distribution map (TNO-GDN; www.dinoloket.nl). Complementary, three cross sections were constructed using TNO's in-house Excel tools for borehole data visualization. The cross-sections illustrate the vertical configuration and internal composition of the terraces and support the identification of terraces limits. The cross-section locations were based on the optimal number of terraces and the availability of good quality borehole descriptions.

The age model used for the terraces is based on Van den Berg (1996) and Van den Berg and Van Hoof (2001), which is mainly based on correlations of paleomagnetic and pollen-based ages with the Quaternary climatic curve.

3.3. Analysis of terrace composition and geometry

Based on the new database, we subsequently analyzed the (i) gravel, gravelly sand, and sand layer thickness ratios (further referred to as composition); (ii) terrace thicknesses; and (iii) terrace longitudinal gradients for each individual terrace and for terrace groups. We calculated the mean value for the compositional and thickness parameters, and associated uncertainties by bootstrapping (see Section 3.3.4). For the longitudinal gradients we applied regression analysis, and the uncertainties were constrained by means of standard error. Further detail on each analysis is provided in the sections below and in Fig. 4.

3.3.1. Lithological composition

We calculated the lithological composition of individual terraces and terrace groups based on the thickness ratio of the lithological classes reported in the borehole logs (Fig. 4). We use three classes: gravel ($\geq \! 30$ % gravel content), gravelly sand ($< \! 30$ % gravel content), and sand layers (0% gravel content). A more detailed subdivision of these classes is not possible.

We first calculated the thickness ratio of each of these three classes in each borehole. In order to prevent depth bias and get the best insight of general composition at each borehole location, we only used boreholes that (i) fully penetrated the terrace sequence (i.e., the base of the borehole reached older sediment layers below the Meuse sequence) *or* (ii) contained a minimal thickness of Meuse sediments of 4 m. The latter selection criterion was applied as otherwise too many boreholes would have to be excluded from the analysis, severely diminishing the general spatial distribution.

Based on the ratios from the individual boreholes, a mean value and its 95 % confidence interval (95 CI) of each class were calculated by bootstrapping it 10×10^3 times (further details in bootstrapping in Section 3.3.4). This process was repeated for both individual terraces and terrace groups.

3.3.2. Terrace thickness

The mean thickness of each terrace was calculated using only the boreholes that fully penetrated the terrace deposits. The terrace thickness was calculated by the difference in elevation of the terrace top and base as recorded in the borehole logs. Careful differentiation was made between terrace deposits and overlying aeolian and colluvial deposits. Finally, the mean thickness of each individual terrace and terrace group was calculated considering every suitable borehole. The mean thickness value and its 95 % confidence interval were calculated by bootstrapping it 10×10^3 times.

3.3.3. Terraces longitudinal gradients

The longitudinal gradient of each terrace was computed relative to the point where the Meuse entered the Netherlands (further referred to as entry point), in the south of the municipality of Eijsden and where the

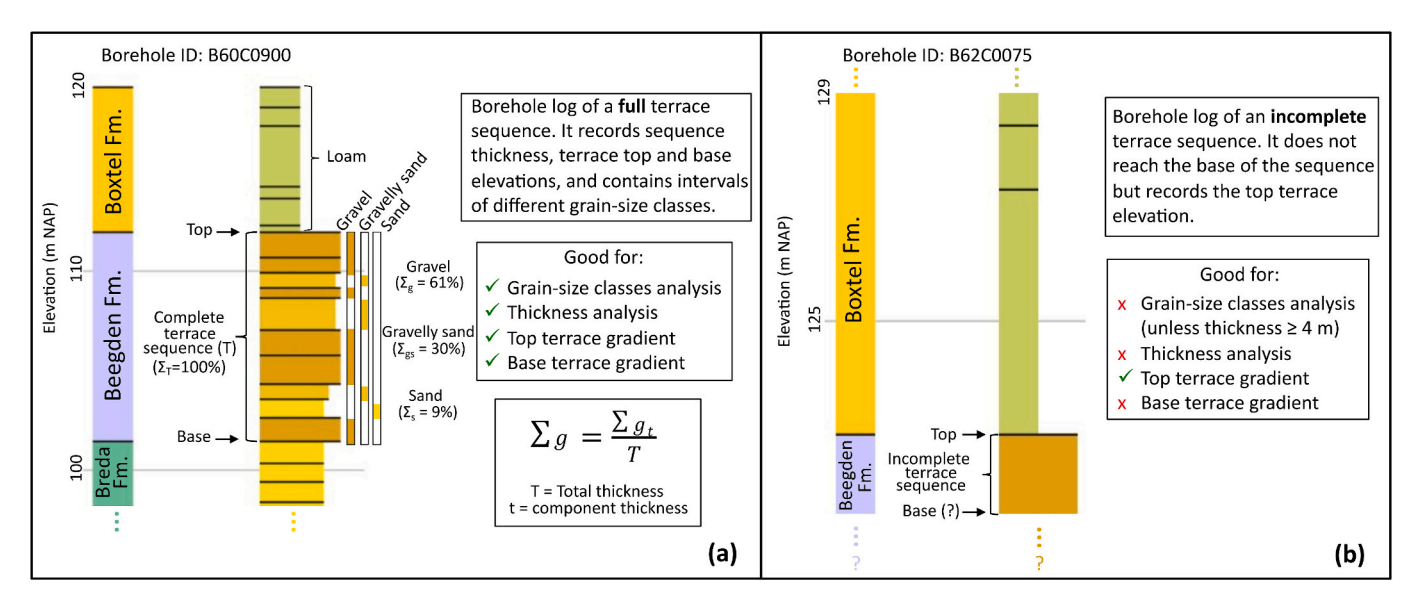


Fig. 4. Illustration of the criteria for defining suitable boreholes for analysis in this study. Examples of borehole logs were obtained from DINOloket (Data and Information on the Dutch Subsurface) in www.dinoloket.nl. Further explanation is found in text (Sections 3.1 and 3.3).

division between East and West Meuse is located (X = 176,400 m; Y = 307,300 m; cf. Van den Berg, 1996). This is the farthest upstream point on the study site, and it is within the area where the terraces start to diverge between East and West Meuse valleys (Fig. 2). The shortest distance from each borehole to the entry point was then calculated. Subsequently, a scatter plot of the distance from the entry point versus the elevation of top and base terrace surface was made. Linear regression was applied to determine a gradient for each terrace. Due to the large scatter in the dataset, all the datapoints deviating above 1 standard-error from the regression line were excluded from further analyses. Then, a new regression line was calculated considering only the datapoints within the 1 standard-error range. The criterion used in the analysis of the top terrace gradient is that the borehole must have at least penetrated the top of the terrace deposits; the criterion used for the base terrace gradient is that the borehole must have penetrated the entire terrace deposit.

Based on the longitudinal gradients, the morphological steps between terraces were calculated. This was done by taking the maximum and minimum height differences between two consecutive top terrace longitudinal gradients. The same process was applied for the terrace base. With these height values, the mean morphological step was calculated.

3.3.4. Bootstrapping

Bootstrapping is a statistical approach that involves constructing simulated datasets by randomly resampling the original dataset with replacement, allowing the possibility of selecting the same data point multiple times. In this approach, simulated datasets are created with the same size as the original dataset. The process involves repeated resampling of the data (typically thousands of times), and, for this study, a total of 10×10^3 resampling was applied for each analysis. Then, the simulated datasets are analyzed regarding their data distribution, in which their central tendency values (e.g., mean, median and mode) and confidence intervals can be calculated. This method is appropriate for cases where the statistical distribution of the dataset is unknown, or nonnormal (non-Gaussian) and when dealing with small sample sizes (Davison and Hinkley, 1997; Helsel et al., 2020). This approach is particularly useful for specific cases where too few samples and large data scatter complicates the calculation of the mean values and associated uncertainties for composition and geometry.

4. Results

4.1. Terrace distribution

Fig. 2 shows the updated terrace map of the study area using the terrace nomenclature of Van den Berg (1989, 1996). The older and highest terrace remnants belong to the East Meuse Terraces Group (red polygons in Fig. 2); they represent seven different terrace levels. These terraces are SW-NE oriented and are paired in their southwestern reaches. In general, they are blanketed by an up to 12-m-thick silty cover (see Kuyl, 1980). Post-depositional erosion caused by secondary drainages is relatively common and has significantly fragmented the terraces remnants, especially the older terraces (i.e., the Kosberg terrace; Fig. 2).

The Higher Terraces (orange polygons, Fig. 2) are composed of ten levels. These terraces belong to the West Meuse Valley and are mostly SSW-NNE oriented and are unpaired, meaning the terraces are not found at the same elevation at both sides of the valley (see Pazzaglia, 2013). The general width of the terraces increases from the upper to the lower ones (from East to West). The maximum width is observed in the St. Pietersberg 2 terrace over the Campine Block on the western flank of the West Meuse valley. The terraces are mostly covered by silt, likely loess deposits, in the south and sandy silt or sand in the north (see Van Haren et al., 2016a). Post-depositional erosion caused by secondary drainages is also common in this group, especially on terraces along the eastern side of the West Meuse Valley. On the western side of the valley, the protecting gravelly Meuse deposits form the Campine Plateau (Beerten et al., 2018).

The Middle Terraces (green polygons, Fig. 2) contain seven terrace levels. These are S-N to SSW-NNE oriented and are also part of the West Meuse valley. These terraces are also mostly unpaired, except for the lower terrace levels, Rothem 2 and Caberg 3, in the reaches of the central and northern part of the study area. In the southern reaches of the Meuse, closer to the Ardennes, the Middle Terraces have narrower widths. On the other hand, in the northern reaches, closer to the subsiding Roer Valley Graben and Feldbiss Fault Zone, the Middle Terraces are wider. In general, these terraces are also covered by silt (likely loess).

Lastly, the young Lower Terraces (blue polygons, Fig. 2), have three levels which are paired in its northernmost reaches. They are also part of the West Meuse valley. The general orientation of these terraces is S-N to SSW-NNE. The terraces in the south are relatively narrow; they become wider closer to the Feldbiss Fault Zone and Roer Valley Graben. Some small patches of Geistingen and Mechelen aan de Maas terraces are

found as erosional remnants in the middle of Holocene deposits. The terraces of the Lower Terraces group are not covered by silt (loess).

4.2. Cross-sections

4.2.1. A-A'

Fig. 5a presents a cross-section over the East Meuse Valley and its

terraces, and a complete figure with the borehole logs and borehole numbers is found in Supplementary Section S1. An up to 10 m thick cover of silt occurs on top of the terraces (including the oldest Saalian, MIS 10, part of the Dutch loess series; Kuyl, 1980). Five different terrace levels have been discriminated in this profile, each separated by 5–10 m high morphological steps. Below, these terraces are presented from high (old) to low (young) with elevation values referring to terrace top.

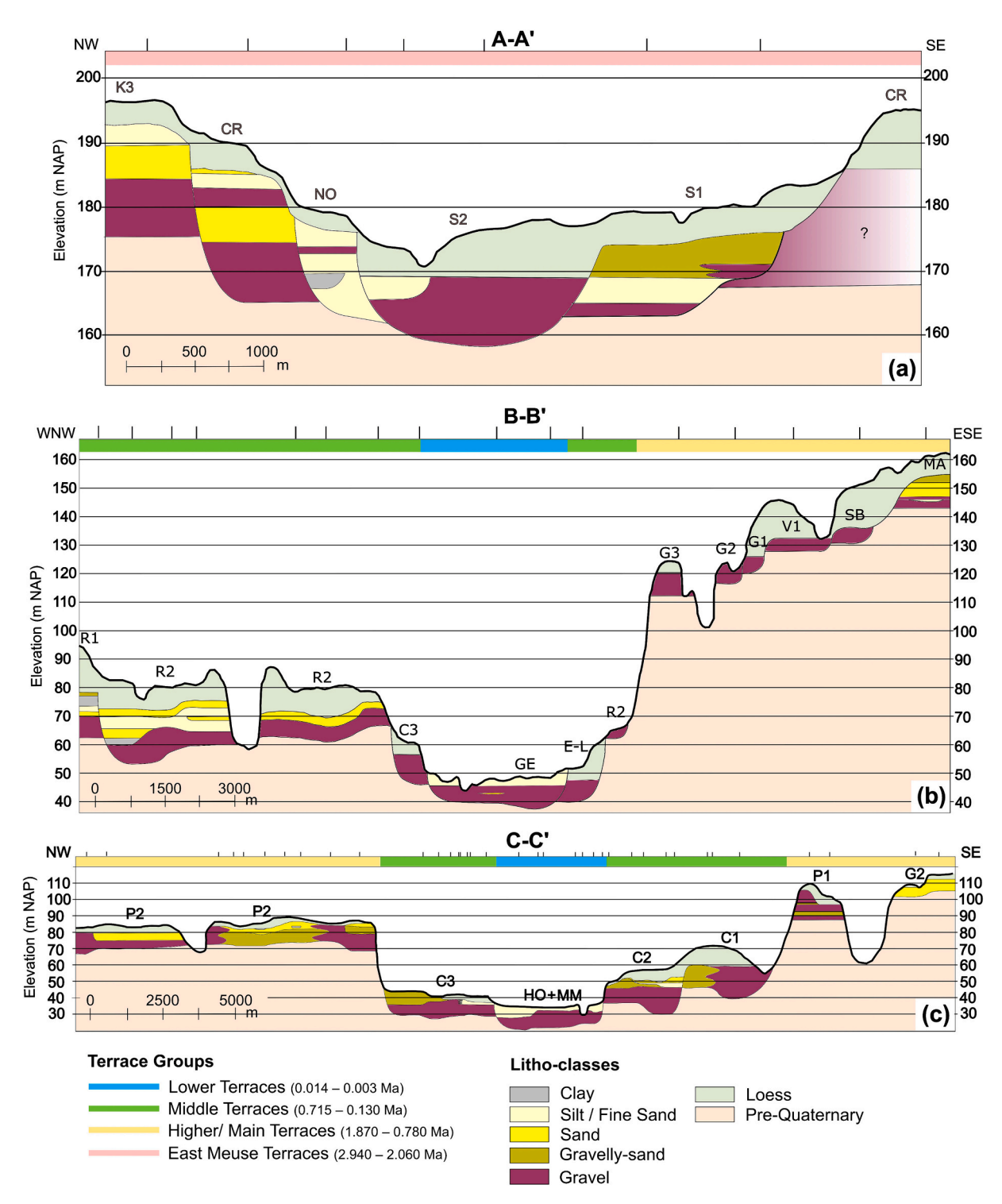


Fig. 5. Cross-sections of the terraces according to location in Fig. 3. (a) Cross-section A–A' across the East Meuse Valley; (b) cross-section B–B' across the West Meuse Valley; (c) cross-section C–C' across the West Meuse Valley. The question mark (?) in the eastern unit of the Crapoel (CR) terrace, in cross-section A–A', refers to inferred composition and thickness based on observations of surrounding boreholes. The pins on top of each cross-section represent the position of boreholes used and can be consulted in Supplementary Figs. S1 and S2. The terrace levels labelling as well as the age span of terrace groups (see Table 1) are after Van den Berg (1996), and Van den Berg and Van Hoof (2001).

Terrace ages can be found in Table 1.

The highest and oldest terrace in this cross-section is Kosberg 3 (K3, see Fig. 5a), with its top surface lying at around 193 m NAP. The associated deposits are about 18-19 m thick. The deposits show a finingupward sequence with a ca. 9-m thick gravel base, followed upward by a 4–5 m-thick sand layer. They are topped by a 2–3 m-thick fine sand/ silty deposit. The next younger terrace is Crapoel (CR; see Fig. 5a), which has its top terrace surface at ca. 186 m NAP. This terrace is paired, and its deposits have a total thickness of about 20 m, showing two fining-upward sequences, in which gravels dominate the total composition. Because there are no borehole data available for the eastern part, the composition at that location was extrapolated using the terrace map and the mean gravelly composition of the East Meuse terraces (see Section 4.3). The next lower terrace level is Noorbeek (NO, see Fig. 5a), lying at ca. 178 m NAP. The associated deposits are about 10-11 m thick. Their composition is dominated by fine sand and silt with a clayey lens within the terrace deposit. The morphological step of 6-7 m separates it from the adjacent lower terrace. Next, Simpelveld 1 terrace is found at ca. 175 m NAP. Its deposits are 10-11 m thick and contain a gravel base of ca. 2 m. Above the gravel layer, a sandy-silt unit is present which laterally grades into a heterogeneous gravelly-sand unit (ca. 4 m thick). The top is composed of gravelly sand. The lowermost and youngest terrace is Simpelveld 2 (S2, see Fig. 5a), at ca. 169 m NAP. The deposits are about 10-m thick, and they are predominantly composed of gravel.

4.2.2. B-B'

Fig. 5b presents a cross section through the southern part of the West Meuse Valley. It is about 18 km long. A thick cover of silt is present in the entire section, reaching up to 10--12 m thick. Twelve different terraces can be discriminated in this profile, separated by morphological steps of 6--10 m. The different elevation values given in the text below refer to the terrace top surface.

The uppermost and oldest terrace is Margraten (MA) at ca. 155 m NAP. The deposits are composed of a 4 m thick gravelly base and overlying 6-7 m thick sand and gravelly sand deposits. The next, lower terrace is Sibbe (SB), separated by a morphological step of about 16-18 m and positioned at 136 m NAP. Its deposits are composed of a 6 m thick gravel layer. The subsequent terrace, separated by a morphological step of about 4 m, is Valkenburg 1 (V1) and is positioned at ca. 132 m NAP. The associated deposits consist of a 4 m thick gravel layer. Sint Geertruid 1 (G1), with a morphological step of about 6 m, follows as the next terrace, at 126 m NAP. This terrace is composed of 6 m thick gravel accumulation. However, this terrace at this location has no borehole data and has been inferred from previous terrace maps and the mean gravel composition (see Section 4.3). The next in the sequence is Sint Geertruid 2 (G2), with a morphological step of about 2 m, at 124-127 m NAP. The terrace deposits are composed of a 6-8 m thick gravel accumulation. The lowermost terrace of the Higher Terraces is Sint Geertruid 3 (G3), with a morphological step of 4-8 m, at ca. 120 m NAP. The deposits are composed of an 8-9 m thick gravel accumulation.

The Middle Terraces is the next group in the sequence. The first Middle Terrace in this cross-section is Rothem 1 (R1), located in the west on the Campine Block. Its top is positioned at 78 m NAP elevation. It is separated from G3 by a steep scarp of ca. 45 m. The terrace deposits are ca. 16 m thick. They contain an 8-m thick gravelly base, followed by silty-sand, silt, and an expressive 4-m thick clayey unit. The subsequent terrace is Rothem 2 (R2), which has its top at ca. 72–75 m NAP. In this location, the thickness of the Rothem 2 terrace deposits varies from 10 to 20 m. It is composed of a gravelly base of 5–9 m thick. The sequences above the base vary laterally in composition, from coarse sand to sandy-clayey sediments. The next terrace is Caberg 3 (C3) at 56 m NAP, which in this section presents an entire 10-m-thick gravel accumulation. On the eastern side of the cross-section, the Eijsden-Lanklaar terrace (EL) is present at around 48 m NAP. Its deposits are entirely composed of gravel and can reach up to 8 m thick. Lastly, the next and lowermost terrace in

this cross section is Geistingen (GE), and it belongs to the Lower Terraces. It is positioned at around 46 m NAP, and its deposits are also mostly composed of gravel, reaching up to 9 m thickness.

4.2.3. C-C'

Fig. 5c presents a cross section across the northern part of the West Meuse Valley. It is about 30 km long. A thick cover of silt (loess) is present throughout the entire section, reaching up to $10-12\,\mathrm{m}$ thick and overlying the terraces. In this section, eight different terraces were identified, which are separated by morphological steps varying from 6 to 8 m. The different elevation values given in the text below refer to the terrace top surface.

The highest terrace is Sint Geertruid 2 (G2), which belongs to the Higher Terraces, and lies at 112 m NAP. In this location, the terrace deposits are 6-8 m thick, and they are composed mainly of sand, with a few admixtures of gravel and silt. Next in sequence comes Sint Pietersberg 1 (P1), which is positioned at 100-105 m NAP. It is mainly composed of gravel and can reach up to 18 m thick. Intercalations of gravel and gravelly sand are observed throughout the terrace sequence. Sint Pietersberg 2 (P2) is the most extensive terrace in this cross section, covering about 9-10 km of the total section length. It is located on the Campine Block at an elevation of around 80–85 m NAP. Its deposits are about 12-14 m thick. They have a gravel base of about 4-5 m thick, but in places the gravel accumulation can reach up to 10 m thickness. A considerable lateral variation in lithology is observed, where the commonly occurring basal gravel gives in to more sandy and gravellysandy sequences in the central part of this terrace section, as evidenced by most boreholes in this specific location. The sandy and gravelly-sandy sequences can vary from 1 to 5 m thick. A scarp of about 40 m height bounds this terrace to lower ones within the inner valley.

The next terrace is Caberg 1 (C1) and belongs to the Middle Terraces. It is positioned at 60 m NAP, and it is composed of up to 20 m thick gravels. The deposits show distinct lateral variation in lithology, changing from gravel to gravelly sand towards the west. Next is the Caberg 2 terrace (C2), which lies at about 50-54 m NAP, and reaches up to 22 m in thickness. It contains a gravelly base of 8-16 m thickness, whereas the upper parts of the deposits are composed of gravelly sand, sand, and some silt near the terrace top. Caberg 3 (C3) is positioned at 40-44 m NAP and its deposits are 10-14 m thick. They are mainly composed of gravel, which can reach up to 10 m thick, but gravelly sand is also present in the upper sequences, reaching up to 8 m thick. Some fine sand and silt are also present. The next terrace belongs to the Lower Terraces and is called Mechelen aan de Maas (MM). It nests part of the Holocene (HO) deposits and is positioned at around 32 m NAP in this location. The base of its deposits is composed of gravel that can reach up to 10 m thick.

4.3. Mean lithological content

4.3.1. Mean gravel content

An increasing trend in the mean gravel content was noticed within the terrace groups (Fig. 6, Table 2). It initially displays a consistent range of around 53 %, within a 95 % confidence interval (CI) between 44 and 61 % (this is referred to as 53 [44–61]%) to 55 [50–60]%, from East Meuse to Higher Terraces. This is followed by a notable increase to 76 [73–79]% within the Middle Terraces, which then progresses to even higher values of 80 [77–84]% in the subsequent Lower Terraces.

Regarding the analysis of individual terraces, a first stage of decreasing mean gravel content is observed in the terraces Kosberg 3 and Crapoel to Noorbeek and Simpelveld 1, from ca. 50 % to ca. 25 % (see Fig. 6 and Table 2 for associated uncertainties). This is followed by a strong increase in the gravel component to ca. 70 % in the terraces Margraten, Sibbe, and Valkenburg 1, followed by a significant decrease to ca. 38 % in Valkenburg 2. Another increase is observed from Sint Geertruid 1 to Sint Geertruid 3, reaching up to and stabilizing around ca. 60 %, and further increasing to up to 83 % in Sint Pietersberg 1. A

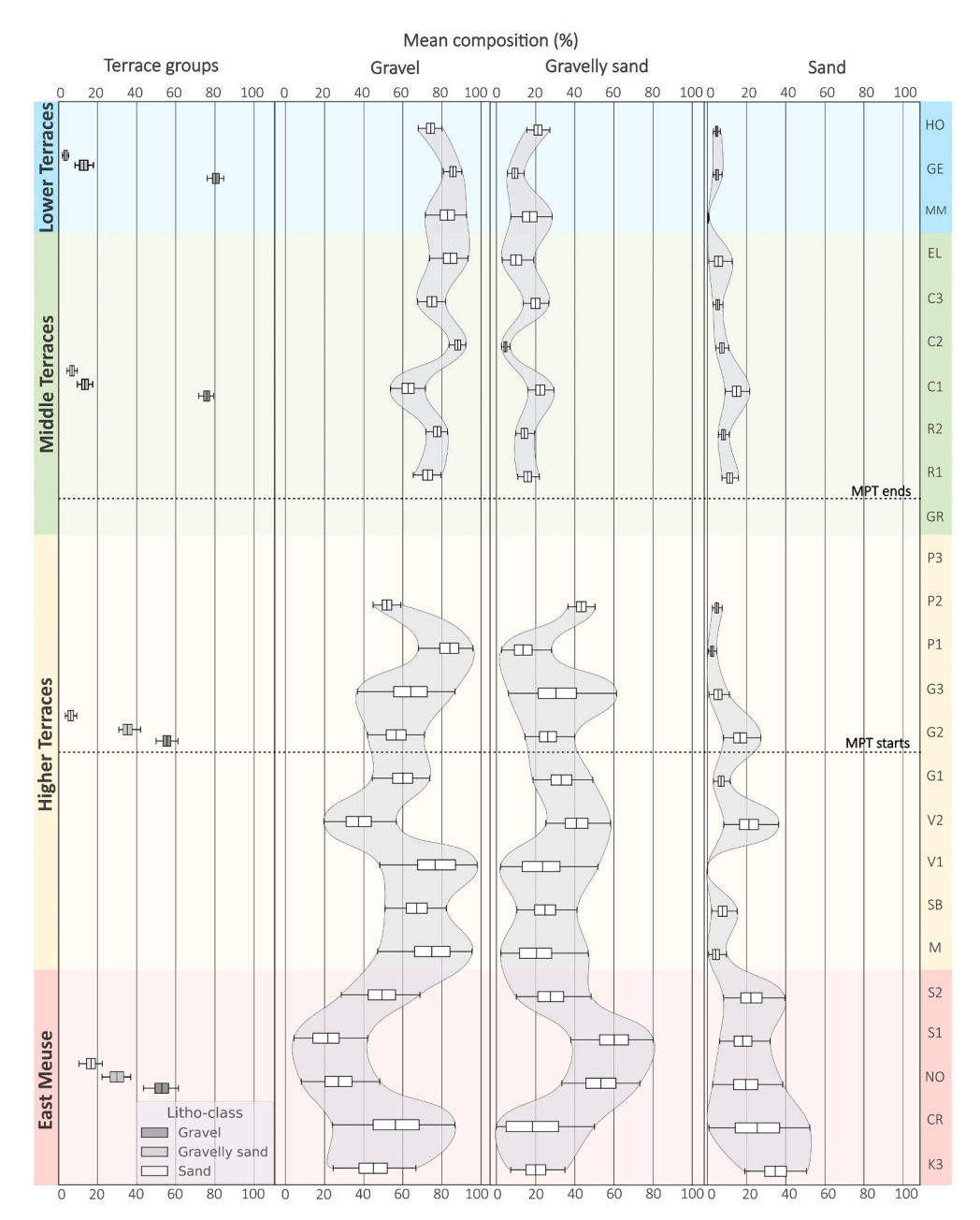


Fig. 6. Boxplot of terraces mean lithological composition and respective 95 % confidence interval (grey shaded area). The plot on the left side represents the mean composition of the terrace groups; dark grey boxes represent gravel content, whilst mid-grey and light-grey boxes represent gravelly-sand and sand contents, respectively. The three other plots each represent litho-class (gravel, gravelly sand, and sand), and display the mean content for each terrace level. Please note that the lines representing the start and end of the MPT are approximations, since these ages vary in the literature (see Clark et al., 2006) Levels Sint Pietersberg 3 (P3) and 's Gravenvoeren (GR) are not included due to lack of data. Complete results are displayed in Table 2.

subsequent decrease to ca. 52 % follows for Sint Pietersberg 2. A gap in the data comes next for terraces Sint Pietersberg 3 and 's Gravenvoeren, due to insufficient borehole data. A relatively steady increase up to ca. 78 % in the gravel content occurs from Rothem 1 to Holocene, with some variability in the Caberg 1-3 terrace series.

4.3.2. Mean gravelly sand content

Terrace group analysis shows a modest increase in the mean gravelly sand content from East Meuse to Higher Terraces, shifting from 30 [22–38]% to 37 [32–42]%. Subsequently, there is a significant decline to 15 [13–18]% and 15 [12–19]% observed for the Middle and Lower Terraces, respectively.

Regarding the analysis of individual terraces, an increase in the gravelly sand component is observed from terraces Kosberg 3 and

Crapoel to Noorbeek and Simpelveld 1, from ca. 19 % to ca. 57 %. A substantial decrease to about 24 % follows, represented by the terraces Simpelveld 2, Margraten, Sibbe, and Valkenburg 1. This is intercalated with a slight increase to ca. 40 % in Valkenburg 2, and decreases again up to ca. 14 %, from Sint Geertruid 1 to Sint Pietersberg 1. A gap in the analysis is present due to lack of data for the Sint Pietersberg 3 and 's Gravenvoeren terraces. A relatively stable gravelly sand content of about 15 % is present from Rothem 1 to the current Holocene floodplain.

4.3.3. Mean sand content

The mean sand content is relatively low for all terrace groups. It drops from 17 [12-23]% for the East Meuse Terraces to 8 [5-10]% and 8 [7-10]% for the Higher and Middle Terraces, respectively. This value then decreases even further to approximately 4 [3-6]% for the Lower

Table 2Terrace mean composition and 95 % confidence interval (CI). Values in bold represent calculations for a terrace group. Terraces Sint Pietersberg 3 (P3) and 's Gravenvoeren (GR) are not included due to lack of data; n = number of observations.

Terrace		Mean composition (%)									
Group	Level	Gravel	Lower 95 CI	Upper 95 CI	Gravelly Sand	Lower 95 CI	Upper 95 CI	Sand	Lower 95 CI	Upper 95 CI	n
Lower	НО	74.2	67.7	80.0	21.2	15.3	27.3	4.7	3.0	6.5	129
	GE	85.6	80.5	90.1	9.5	5.5	14.0	4.9	2.8	7.4	152
	MM	82.6	71.2	92.4	17.2	7.1	28.4	0.3	0.0	0.8	33
	Lower	80.5	76.8	84.0	15.1	11.6	18.6	4.4	3.1	5.7	314
Middle	EL	84.0	73.3	93.3	10.2	2.7	19.0	5.8	0.7	12.7	42
	C3	74.8	67.3	81.8	20.0	13.6	26.7	5.3	3.0	7.9	85
	C2	88.0	83.6	92.1	4.6	2.5	6.9	7.4	4.2	10.9	41
	C1	62.7	53.5	71.5	22.4	16.1	29.3	14.9	9.0	21.5	47
	R2	77.5	71.7	82.7	14.3	9.8	19.4	8.2	5.6	11.2	103
	R1	72.6	65.1	79.4	16.0	10.8	21.9	11.4	7.4	15.8	54
	GR	-	_	_	_	_	_	_	_	_	-
	Middle	76.2	73.0	79.1	15.3	12.8	17.9	8.5	6.9	10.2	372
Higher	P3	_	_	_	_	_	_	_	_	_	_
Higher	P2	51.9	44.6	58.9	43.4	36.3	50.4	4.8	2.5	7.5	136
	P1	83.5	67.7	95.8	14.0	2.5	28.1	2.4	0.4	4.8	18
	G3	63.5	36.5	86.7	31.3	3.6	61.3	5.5	0.7	11.2	7
	G2	56.6	41.6	71.1	26.5	14.3	40.0	16.9	8.0	27.3	30
	G1	59.8	43.9	73.8	33.2	18.4	49.2	7.0	3.0	11.6	26
	V2	37.6	19.3	56.6	41.1	24.8	58.3	21.5	8.1	36.4	18
	V1	76.4	48.2	97.9	23.6	0.0	51.8	0.0	0.0	0.0	8
	SB	67.0	50.7	82.2	25.0	10.1	41.2	7.9	2.1	15.2	17
	M	74.5	46.4	95.4	20.7	0.0	46.8	4.5	0.3	9.7	9
	Higher	55.2	49.7	60.6	37.1	31.9	42.2	7.7	5.4	10.1	269
East Meuse	S2	49.2	28.2	68.7	27.9	9.8	48.3	22.7	8.1	39.5	16
East Meuse	S1	21.8	4.3	42.0	59.9	37.4	80.0	18.3	6.1	32.0	11
	NO	27.2	8.1	48.3	53.3	33.4	73.2	19.4	2.6	38.5	5
	CR	56.3	23.2	86.6	18.2	0.0	50.0	25.7	0.8	52.3	6
	К3	45.0	24.0	66.6	20.2	6.9	35.0	34.8	18.7	50.6	13
	East Meuse	53.0	44.2	61.5	29.9	22.2	37.8	17.0	11.7	22.7	51

Terraces.

The sand component decreases substantially from Kosberg 3 to Valkenburg 1, from ca 35 % to 0 %. It then shows a more oscillatory behavior, abruptly increasing to up to ca. 20 % in Valkenburg 2, and alternating between ca. 17 and 3 %, from Sint Geertruid 1 to Sint Pietersberg 2. A gap in the data follows due to the lack of available data for terraces Sint Pietersberg 3 and 's Gravenvoeren, subsequently presenting a more stable mean sand content of around 7 %, from terrace level Rothem 1 to the current Holocene floodplain.

4.4. Mean terrace thickness

The terrace groups analysis shows a slight increasing trend in thickness. The terraces display an initial and minimum mean thickness of 6.9 [6.0-7.9] m for the East Meuse, which subsequently rises to 9.2 [8.5-9.9] m for the Middle Terraces. Then, it modestly decreases to 8.3 [7.9-8.7] m for the Lower Terraces. The analysis of individual terrace thicknesses does not display any clear long-term trend. Furthermore, the individual terraces yielded significant variations (Fig. 7, Table 3). The mean thickness of the individual terraces varies between 5.4 [4.0-7.0] m (Sibbe terrace) and 13.1 [11.7-14.4] m (Caberg 1 terrace). The confidence intervals are larger for the older terraces due to the limited number of observations (Table 3). Despite the rather large uncertainties, a steady but very slight decreasing trend of the mean terrace thickness is observed from Simpelveld 1 to Valkenburg 1, which shows a decrease of about 3 m. Then, an "abrupt" increase of about 4-5 m follows in the level Valkenburg 2, reaching a thickness of 10.1 [7.2–13.0] m. Subsequently, the mean thickness decreases and becomes rather steady around 8 m from terraces Sint Geertruid 1 to Rothem 2. Another "abrupt" increase is observed reaching a maximum mean thickness of 13.1 [11.7–14.4] m for Caberg 1. It then decreases to 10.3 [7.8-12.8] m for Caberg 2 and reaches a certain stability of around 8 m thick, from Caberg 3 to Mechelen aan de Maas. Finally, a slight increase to 9.3 [8.8-9.7] m in the level Geistingen is observed and followed by a decrease to 6.6 [5.9-7.2] m for the current Holocene floodplain.

4.5. Gradients of the terraces

Both the terrace top and terrace base gradients of each terrace level were calculated (Fig. 8 and Table 4). Fig. 9 a and b display the longitudinal profiles of the reconstructed gradients for terraces top and base. A more detailed explanation about these gradients is found in Supplementary Section S2, Fig. S3, and Table S1.

In general, longitudinal profiles of the East Meuse terraces and some of the Higher Terraces have a more limited length, ranging from 3 to 15 km. The longest profile is Sint Pietersberg 2, which is about 35 km long, due to its extension over the Campine Block (see Figs. 1 and 2). However, the Lower Terraces, especially the Holocene level, are the most continuous in extension.

Overall, the East Meuse Terraces present reversed gradients, whereas the other (younger) groups present normal gradients dipping towards the current flow direction of the Meuse, although a few exceptions are present (Figs. 8, 9, and Table 4). A maximum terrace top reversed gradient of 6.80 ± 0.33 m/km (uncertainty equal to one standard error) was found for the Noorbeek terrace, and a minimum of 0.11 ± 0.18 m/km for the Simpelveld 2 terrace. The normal gradients of the terrace tops show a maximum of 4.18 ± 0.89 m/km for the Valkenburg 2 terrace, and a minimum of 0.04 ± 0.15 m/km for the Eijsden-Lanklaar level. Overall, the levels of the Middle and Lower Terraces are sub-parallel to each other, except for Eijsden-Lanklaar due to its nearly flat gradient.

Regarding the terrace base reversed gradients, terrace Noorbeek presents the maximum value of 23.56 ± 6.24 m/km, and Sint Geertruid 3 has the minimum value of 0.18 ± 0.67 m/km. For the normal base gradients, Crapoel holds the maximum of 12.26 ± 14.56 m/km (Table 4), while Eijsden-Lanklaar displays the minimum of 0.39 ± 0.16 m/km (Figs. 8 and 9, and Table 4).

The base terrace longitudinal profiles present a similar pattern as the top terrace longitudinal profiles (Figs. 8, 9 and Table 4). The East Meuse

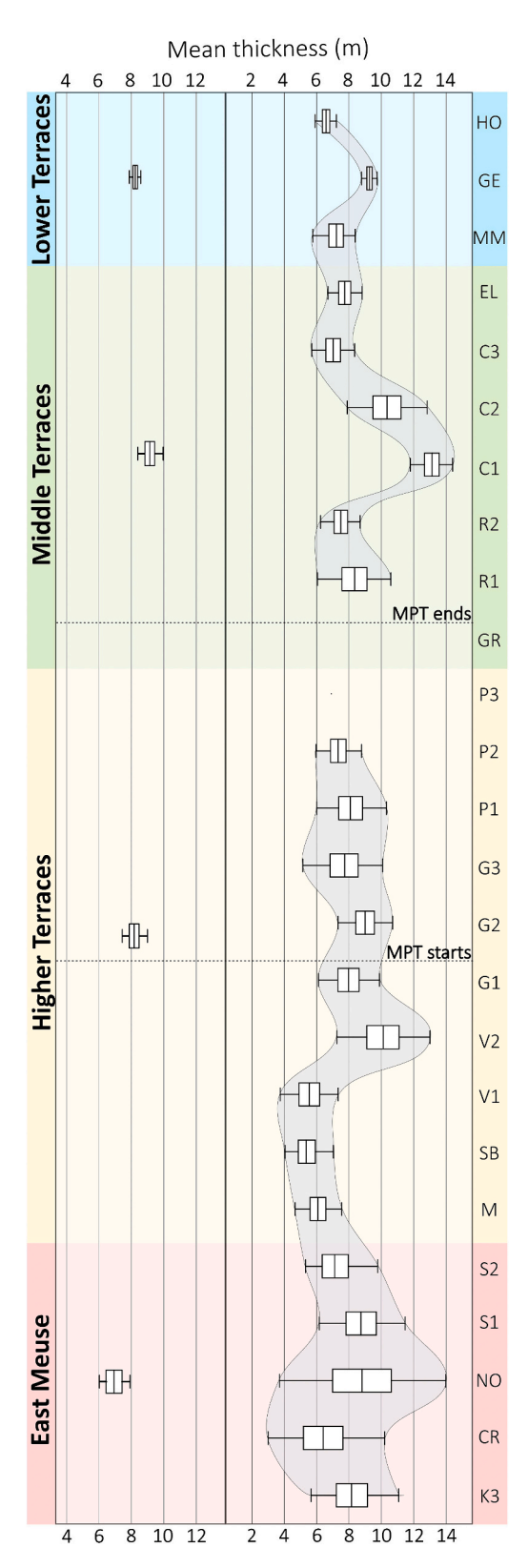


Fig. 7. Boxplot of terrace mean thicknesses and respective 95 % confidence interval (grey shaded area). The plot on the left side represents the mean thickness of each terrace group. The plot on the right side represents the mean thickness of each terrace level. Please note that the lines representing the start and end of the MPT are approximations, since these ages vary in the literature (see Clark et al., 2006) Levels Sint Pietersberg 3 (P3) and 's Gravenvoeren (GR) are not included due to lack of data. Complete results are displayed in Table 3.

Table 3 Mean terrace thickness and 95 % confidence interval (CI). Values in bold represent calculations for a terrace group. Terraces Sint Pietersberg 3 (P3) and 's Gravenvoeren (GR) are not included due to lack of data; n= number of observations.

Terrace		Mean thickness (m)							
Group	Level	Thickness	Lower 95 CI	Upper 95 CI	n				
Lower	НО	6.6	5.9	7.2	63				
	GE	9.3	8.8	9.7	127				
	MM	7.2	5.7	8.4	16				
	Lower	8.3	7.9	8.7	206				
Middle	EL	7.7	6.7	8.8	40				
	C3	7.0	5.7	8.3	26				
	C2	10.3	7.8	12.8	20				
	C1	13.1	11.7	14.4	45				
	R2	7.5	6.2	8.7	40				
	R1	8.3	6.0	10.6	10				
	GR	-	_	_	_				
	Middle	9.2	8.5	9.9	181				
Higher	P3	_	_	_	-				
	P2	7.3	5.9	8.8	59				
	P1	8.1	6.0	10.3	16				
	G3	7.7	5.1	10.1	7				
	G2	9.0	7.3	10.7	29				
	G1	8.0	6.1	9.9	22				
	V2	10.1	7.2	13.0	15				
	V1	5.5	3.7	7.3	10				
	SB	5.4	4.0	7.0	17				
	M	6.1	4.6	7.5	9				
	Higher	8.1	7.3	9.0	184				
East Meuse	S2	7.2	5.3	9.8	17				
	S1	8.8	6.1	11.5	10				
	NO	8.8	3.7	14.0	6				
	CR	6.4	3.0	10.2	5				
	К3	8.2	5.6	11.1	11				
	East Meuse	6.9	6.0	7.9	49				

Terraces are mostly reversed, except for Simpelveld 1 and Crapoel. The Higher Terraces present normal gradients, except for Margraten, Valkenburg 1 and Sint Geertruid 3. The Middle and Lower terraces also present a parallel to sub-parallel setting, except for Rothem 1, which is reversed.

Morphological steps between terraces were calculated from the longitudinal profile (Fig. 9c). The maximum step from top terrace to top terrace of ca. 16 m was identified between the Sibbe and Valkenburg 1 terrace levels, whereas the minimum step of ca. 1 m is between terraces Mechelen aan de Maas and Geistingen.

5. Discussion

In Fig. 10 we show a synthesis of our analysis results on gravel-sand ratios, terrace deposit thickness, gradient and incision plotted next to the northwest European Quaternary chronostratigraphic scheme and paleomagnetic record (Cohen and Gibbard, 2019), and the deep-ocean oxygen isotope record (Marine Isotope Stages — MIS; Lisiecki and Raymo, 2005). We plotted our results using the Meuse terrace age framework of Van den Berg (1996) and Van den Berg and Van Hoof (2001). Although there are dating limitations and uncertainties for this age model (especially for the older terraces), which complicate direct correlations of specific terraces to MIS stages, (see Table 1) our results show clear overall temporal trends. Below we discuss our results in relation to the long-term climatic developments shown in Fig. 10.

5.1. Tectonic control

At least three different tectonic processes control the tectonic motions in the study area: Alpine folding since the start of the Neogene, domal plume uplift since the Middle Pleistocene centered around the volcanic Eifel area, and vertical motions associated with faulting along the southern boundary faults of the Roer Valley Rift System (Van Balen

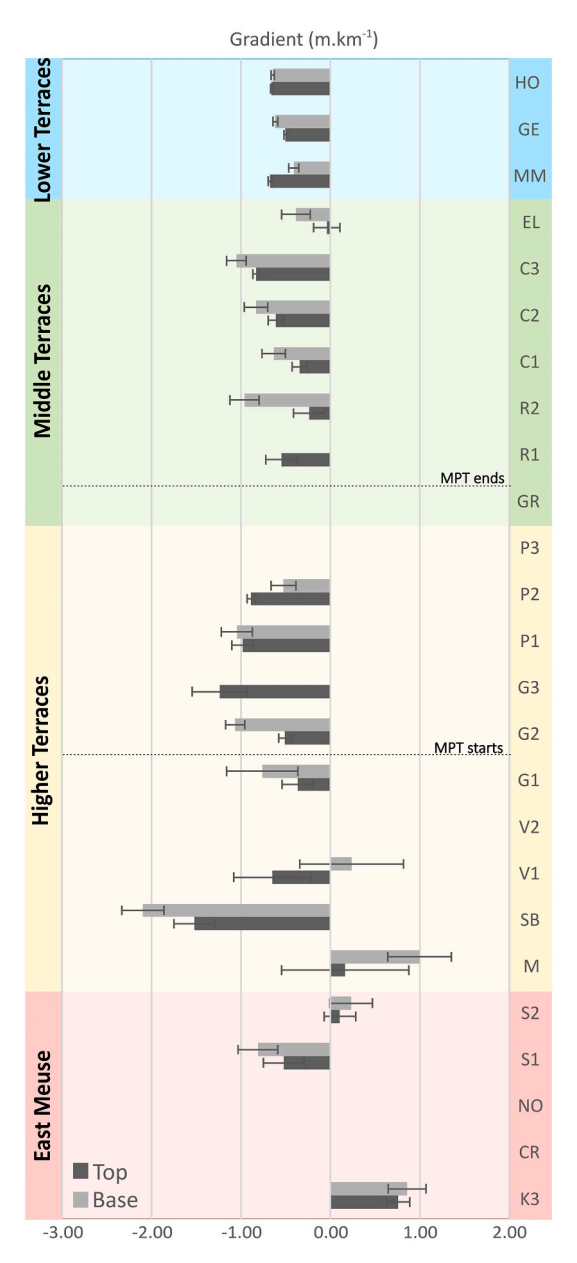


Fig. 8. Terrace top and base gradients and their respective standard errors. Gradients $<0~{\rm km\cdot m^{-1}}$ are dipping downstream, whereas gradients $>0~{\rm m\cdot km^{-1}}$ are reversed. Please note that the lines representing the start and end of the MPT are approximations, since these ages vary in the literature (see Clark et al., 2006). Levels Sint Pietersberg 3 (P3) and 's Gravenvoeren (GR) are not included due to lack of data. The following terraces are not included due to sparse data or implausible gradients: top terraces Noorbeek (NO) and Valkenburg (V2), and base terraces Crapoel (CR), Noorbeek (NO), Valkenburg 2 (V2), Sint Geertruid 3 (G3) and Rothem 1 (R1); The complete result of the gradient analysis is found in Table 4. Further information on this dataset is found on the Supplementary Material Section S2, Fig. S3 and Table S1.

et al., 2000; Michon and Van Balen, 2005; Demoulin and Hallot, 2009). Our analysis indicates that the East Meuse terrace gradients are low or reversed (Figs. 8 and 9), opposite to the paleo-flow direction. In addition, the terraces in the East Meuse valley are paired, indicating a lack of substantial tilting in a northern direction during their formation. Alpine folding thus had limited impact. Therefore, the most likely tilting mechanism affecting the terrace gradients seems to be footwall backtilting in response to faulting along the Feldbiss Fault Zone (see Fig. 1; Leeder and Gawthorpe, 1987; Thompson and Parsons, 2016).

The East Meuse valley was abandoned during the late Tiglian

regional stage in favor of the West Meuse Valley (Kuyl, 1980; Van den Berg and Van Hoof, 2001), although a younger age of abandonment was also suggested (Westerhoff et al., 2008). In addition to footwall back tilting, capturing by a local south-north drainage system, which were common during the Early-Pleistocene in the southern Netherlands (Stramprov Formation; Kasse, 1988; Westerhoff et al., 2008) is plausible. The capture indicates a steeper gradient towards the north, which is an indication for northward tectonic tilting, in line with the Alpine folding uplift. Furthermore, the observed increase in gravel content at the transition from East Meuse to West Meuse Higher Terraces (Figs. 6 and 10) could be related to this capture event. The new and steeper path would likely increase the Meuse transport capacity enhancing transport of gravel-sized particles. A possibly contributing factor to the capture is karstic processes, as the shallow subsurface lithology consists predominantly of Cretaceous limestone. Similarly, the capture of the headwaters of the Meuse by the Moselle river (northeastern part of the Paris Basin) has been explained by karstic processes (Losson and Quinif, 2001).

In the West Meuse Valley, the Meuse gradually migrated westward, indicated by the asymmetry of the terraces and by unpaired terraces preserved on the eastern flank of the valley. This pattern of migration can be attributed to the folding by Alpine compression and by plume-induced uplift, producing the general northwestward tilting observed in the region. The oldest part of the Higher Terrace record shows that significant incision occurred (M/SB and SB/V1 morphological steps in Fig. 9). Westward lateral migration culminated during deposition of the Sint Pietersberg 2 terrace that formed around ca. 0.9 Ma (the late Bavelian regional stage; Fig. 10).

Following the formation of the Sint Pietersberg 2 terrace, the Meuse (re)established a course towards the central part of the West Meuse valley. It strongly incised, with a maximum incision occurring between the formation of the Sint Pietersberg 3 and 's Gravenvoeren terraces (see Van Balen et al., 2000; Schaller et al., 2004; Rixhon and Demoulin, 2018), hereby forming the Middle and Lower Terraces (Fig. 10). This course direction and onset of strong incision is linked to the effect of plume-induced domal uplift (Van Balen et al., 2000) and to enhanced fault displacement in the Roer Valley Graben (see Kasse, 1988; Houtgast and Van Balen, 2000; Gold et al., 2017). The incision is partially reflected in the morphological steps displayed in Fig. 9c and marks the transition between the High and Middle terraces. The cross sections B-B' and C-C' (Fig. 5b and c) indicate that incision during formation of the Middle and Lower Terraces accelerated and reached a total of ca. 40 m. The inferred lateral migration and incision are accompanied by an overall decrease of terrace gradients of the Higher to the Middle/Lower Terraces with the exception being the levels Caberg 2 and 3, which are relatively steep (Figs. 8 and 9). The general decrease in the gradient shows that tilting occurred during terrace staircase formation, steepening the older terrace gradients.

5.2. Climatic control

The increase in the mean gravel content and decrease in gravelly sand and sand content in the terrace sequence is in line with the enhanced physical weathering and erosional processes in the Meuse catchment resulting from the Quaternary climate cooling and associated increase of the climate cycle amplitude (Figs. 6 and 10). However, surprisingly, our findings show only a small increase in the mean thickness of the terraces in the terrace groups (Figs. 7 and 10).

5.2.1. East Meuse

A significant compositional difference is present between the East Meuse Terraces and the Higher, Middle and Lower Terraces of the West Meuse (Figs. 6 and 10). A higher amount of sand and gravelly sand is present compared to the younger terrace groups. A potential explanation is the erosion of the Ardennes weathering mantle (Tesch, 1941; Demoulin et al., 2018). This overburden consists of fine-grained material, probably a product of the Early Miocene (sub)tropical weathering

Table 4
Terraces top and base gradients and respective uncertainties. Gradients $< 0 \text{ km} \cdot \text{m}^{-1}$ are dipping downstream, whereas gradients $> 0 \text{ m} \cdot \text{km}^{-1}$ are reversed. Terraces Sint Pietersberg 3 (P3) and 's Gravenvoeren (GR) are not included due to lack of data; n = number of observations.

Terrace		Top gradient					Base gradient					
Group	Level	Gradient (m·km ⁻¹)	Gradient std. error (m·km ⁻¹)	Regression line std. error (m)	\mathbb{R}^2	n	Gradient (m·km ⁻¹)	Gradient std. error (m·km ⁻¹)	Regression line std. error (m)	R^2	n	
Lower	НО	-0.66	0.01	1.14	0.95	211	-0.65	0.02	1.16	0.97	45	
	GE	-0.51	0.02	0.99	0.87	161	-0.62	0.03	1.24	0.84	100	
	MM	-0.68	0.02	1.24	0.96	55	-0.41	0.06	0.58	0.86	10	
Middle	EL	-0.04	0.15	2.25	0.00	32	-0.39	0.16	2.35	0.19	26	
	C3	-0.83	0.04	2.34	0.83	115	-1.05	0.11	2.00	0.91	11	
	C2	-0.61	0.08	2.13	0.77	18	-0.83	0.13	2.37	0.80	12	
	C1	-0.35	0.08	2.90	0.35	34	-0.63	0.13	2.81	0.43	33	
	R2	-0.24	0.17	3.04	0.02	84	-0.96	0.16	3.05	0.63	20	
	R1	-0.55	0.18	2.25	0.18	48	1.62	0.11	0.41	0.99	5	
	GR	_	_	_	_	_	_	_	_	_	-	
Higher	P3	_	_	-	_	_	_	_	_	_	_	
	P2	-0.89	0.05	4.93	0.53	345	-0.52	0.14	3.26	0.36	27	
	P1	-0.98	0.12	2.10	0.86	13	-1.05	0.17	2.61	0.80	11	
	G3	-1.24	0.31	2.01	0.84	5	0.18	0.67	2.69	0.02	5	
	G2	-0.51	0.07	2.57	0.70	27	-1.07	0.11	2.38	0.88	16	
	G1	-0.37	0.17	3.65	0.21	19	-0.76	0.40	5.51	0.27	12	
	V2	-4.18	0.89	3.57	0.65	14	-5.31	1.85	5.68	0.54	9	
	V1	-0.65	0.43	1.85	0.31	7	0.24	0.58	2.39	0.04	6	
	SB	-1.52	0.23	2.01	0.80	13	-2.10	0.24	1.45	0.92	9	
	M	0.16	0.71	2.01	0.01	7	1.00	0.35	0.75	0.73	5	
East	S2	0.11	0.18	3.38	0.03	14	0.23	0.24	4.09	0.10	11	
Meuse	S1	-0.52	0.23	3.86	0.43	9	-0.81	0.22	3.01	0.77	6	
	NO	6.80	0.33	0.36	1.00	4	23.56	6.24	1.80	0.93	3	
	CR	0.62	0.57	4.92	0.28	5	-12.26	14.56	10.17	0.41	3	
	КЗ	0.76	0.13	2.92	0.78	12	0.86	0.21	3.20	0.85	5	

in the Ardennes and sediments deposited by the Oligocene and Miocene marine transgressions over the Ardennes massif (Demoulin, 1995; Demoulin et al., 2018). Therefore, the East Meuse terraces also have a high quartz and stable heavy mineral content, which decreases with time (Van Straaten, 1946; Zonneveld, 1949; Bustamante-Santa Cruz, 1973).

5.2.2. West Meuse

The increased gravel content observed in the Higher Terraces, and particularly in the Middle and Lower Terraces (Figs. 6 and 10), can be attributed to the increased erosion in the Ardennes and enhanced transport capacity. As climate deteriorated during the Pleistocene with longer and deeper glacial cycles, fresh and/or partially weathered rocks were exposed and eroded during the cold periods. In addition, peak discharges were likely higher, especially during the snow-melt water season, sustaining increased capacity to erode and transport gravelly sediments. Another potential explanation for the gravel content increase over time concerns the gradual progradation of the Meuse gravel front (see Section 5.4.).

Regarding the mean terrace thickness of the terrace groups, a slight increasing trend is observed from East Meuse Terraces to Middle Terraces, from 6.9 [6.0, 7.9] m to 9.2 [8.5, 9.9] m (Fig. 7 and Table 3). However, this trend is not clear in the mean thickness of individual terraces. The general trend may be in line with the Quaternary climate cooling and associated increase of the climate cycle amplitude, leading to enhanced erosion and periglacial weathering, which likely increased sediment production in the Ardennes. Schaller et al. (2004) demonstrated that catchment-averaged paleo erosion rates of the Meuse were rather stable around 25-35 mm/kyr from ca. 1.3 to 0.7 Ma but increased to 30–80 mm/kyr after 0.7 Ma. The increased paleo erosion rates may be reflected in the increase in thickness as observed in the Middle Terraces (9.2 [8.5, 9.9] m). However, this value is significantly influenced by the Caberg 1 mean thickness of 13.1 [11.7, 14.4] m. Excluding this data from analysis, the Middle Terraces mean thickness is around 8.2 m, which is as thick as the Higher and Lower Terraces.

The large thickness values observed in the terraces Caberg 1 (13.1 [11.7, 14.4] m) and, to some extent, Caberg 2 (10.3 [7.8, 12.8] m), point

towards exceptional conditions (Figs. 7 and 10, Table 3). Based on the age model employed in this study, Caberg 1 was likely formed during the Elsterian glaciation (MIS 12), a major glacial period marked by the substantial advance of ice sheets into the European continent and the northern Netherlands (Ehlers et al., 2018). The Elsterian stage presents one of the largest climatic oscillations according to the oxygen isotope record for the Quaternary (Fig. 10). Following the findings of Yuan et al. (2022), this could mean that the amplitude of the cold-climate oscillation was maximal and the uplift rates in the source area were high enough to increase sediment input, particularly of coarse-grained sediment.

5.3. Imprints of the Mid-Pleistocene Transition

Our findings show that during the Mid-Pleistocene Transition (MPT) the mean gravel content increased, while mean terrace thickness shows a weak increase (Fig. 10). These long-term trends seem to be more reasonably related to the overall Quaternary climate cooling than the MPT. Figs. 6 and 10 show that the gravel content increase starts to be noticeable around 2.0 Ma with the formation of the Simpelveld 2 terrace, and consolidates around 0.6 Ma (Mid-Cromerian, MIS 16), evidenced by the Rothem 1 terrace. In other words, the increase in gravel content started ca. 0.8 Myr before and ended ca. 0.1 Myr after the MPT.

However, if we consider the MPT as part of the general Quaternary climate cooling, a correlation is reasonable. Similarly, the peaks observed in mean terrace thickness of the levels Valkenburg 2 and Caberg 1 (Figs. 6 and 10) are respectively older and younger than the time interval of the MPT, whereas the mean thickness of syn-MPT terraces is relatively constant.

Alternatively, if the discernible increase in the gravel content during the transition from East Meuse to Higher Terraces is due to a capture event (see Section 5.1), it becomes plausible that the oscillations in gravel content observed in some of the syn-MPT terraces (G2, G3, P1, and P2 in Fig. 10) may represent a transient period. This assumption is based on the gradual nature of the MPT, where a transient signal indicative of the changes from 40-ky to 100-ky cycles could plausibly be

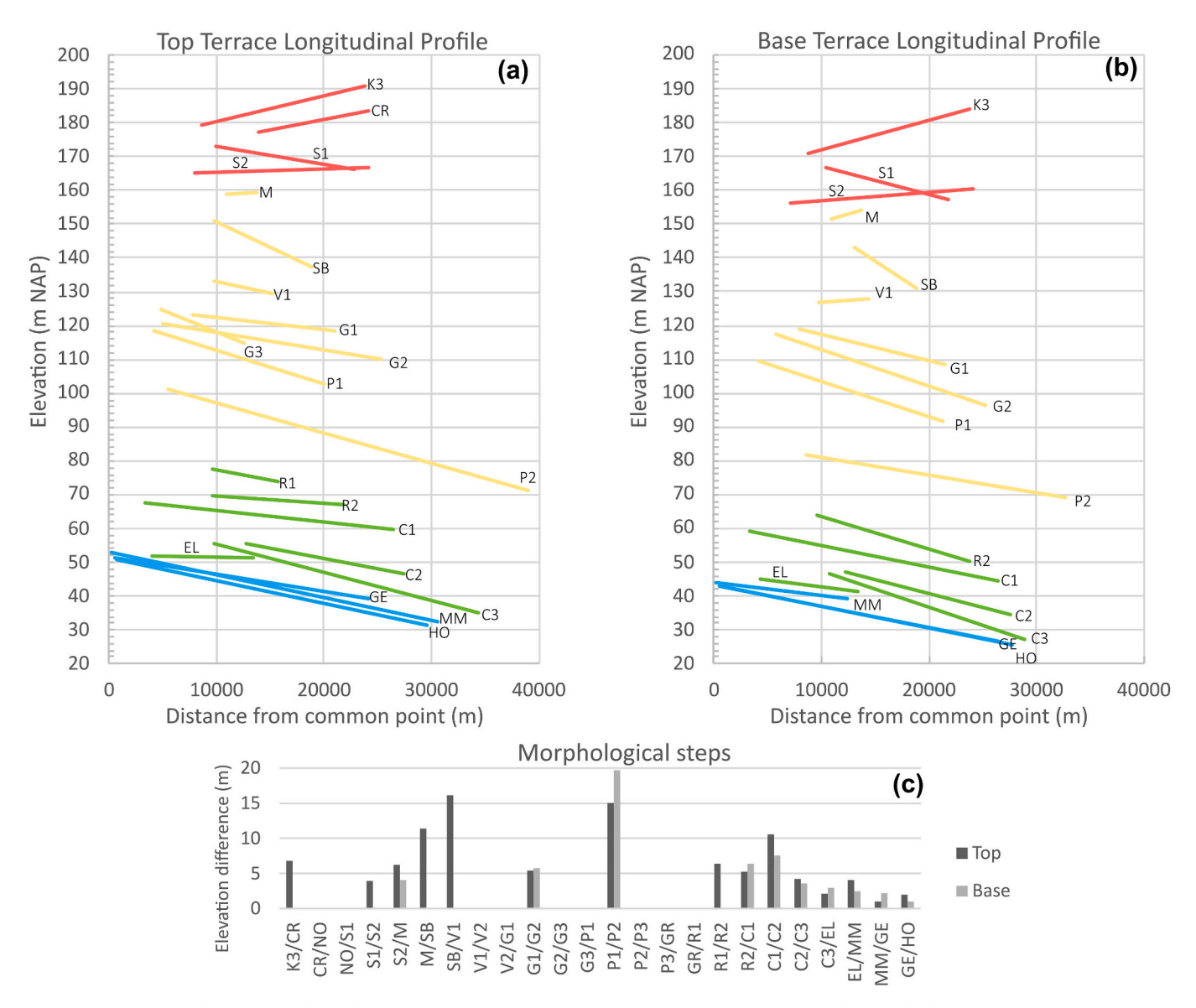


Fig. 9. Longitudinal profile and morphological steps of top and base terraces. (a) Longitudinal profile reconstructed using the elevation of the top terrace for each terrace level; (b) Longitudinal profile reconstructed using the elevation of the base terrace for each terrace level; (c) Morphological steps calculated from the difference from top terrace to the immediate next top terrace (e.g., K3/CR, from Kosberg 3 to Crapoel) and from base terrace to the next base terrace; Terrace Sint Pietersberg 3 (P3) and 's Gravenvoeren (GR) are not included due to lack of data. The following terraces are not included due to sparse data or implausible gradients: top terraces Noorbeek (NO) and Valkenburg (V2), and base terraces Crapoel (CR), Noorbeek (NO), Valkenburg 2 (V2), Sint Geertruid 3 (G3) and Rothem 1 (R1); Note that there is no crosscutting relationship between the terraces; the apparent crosscutting is due to the regression statistics applied and to the considerable uncertainties. The complete result of this analysis, including data not showed in this figure, is found in Table 4. Further information on this dataset is found on the Supplementary Material Section S2, Fig. S3 and Table S1.

translated into an oscillating signal of gravel content. Once the 100-ky cycle finally consolidates, indicating the end of the MPT, the high gravel content stabilizes, as observed in the Middle and Lower Terraces.

Gibbard and Lewin (2009) attributed enhanced valley incision of several European rivers systems to the MPT. Increased incision is observed in the Meuse terrace record at the transition from the Higher to the Middle Terraces, marked by a large-scale morphological convexity in the West Meuse valley (see Fig. 5). However, the MPT (ca. 1.25–0.65 Ma) started well before the incision phase after Sint Pietersberg 3 (0.78 Ma). In addition, the transition from Higher to Middle Terraces is abrupt, whereas the MPT is gradual. Also, this increased incision has been explained by plume-induced uplift in the Eifel region, for which independent evidence exists (Van Balen et al., 2000; Schaller et al., 2004).

Despite the major impact on sea-level related to the Quaternary

climate changes, base-level changes probably did not affect or had limited influence on the formation and preservation of the Meuse terraces due to the large distance to the coastline. According to Van Balen et al. (2000), the approximate distance from the coastline to the Ardennes front (study area) is, respectively, about 200 km and 1000 km during sea level high- and low-stands. Also, the Meuse longitudinal gradient between this 200 and 1000 km is not much different from the current lower Meuse. Furthermore, as demonstrated by Tebbens et al. (2000), the sea-level changes during the Holocene and Eemian may have affected fluvial dynamics up to the Meuse reaches on the Venlo Block and downstream part of Roer Valley Graben (ca. 110 km from the current coastline). This suggests that the Meuse terraces in the study area (ca. 200 km from the current coastline) are rather insensitive to sea-level changes.

In summary, our findings indicate that a clear MPT signal in the

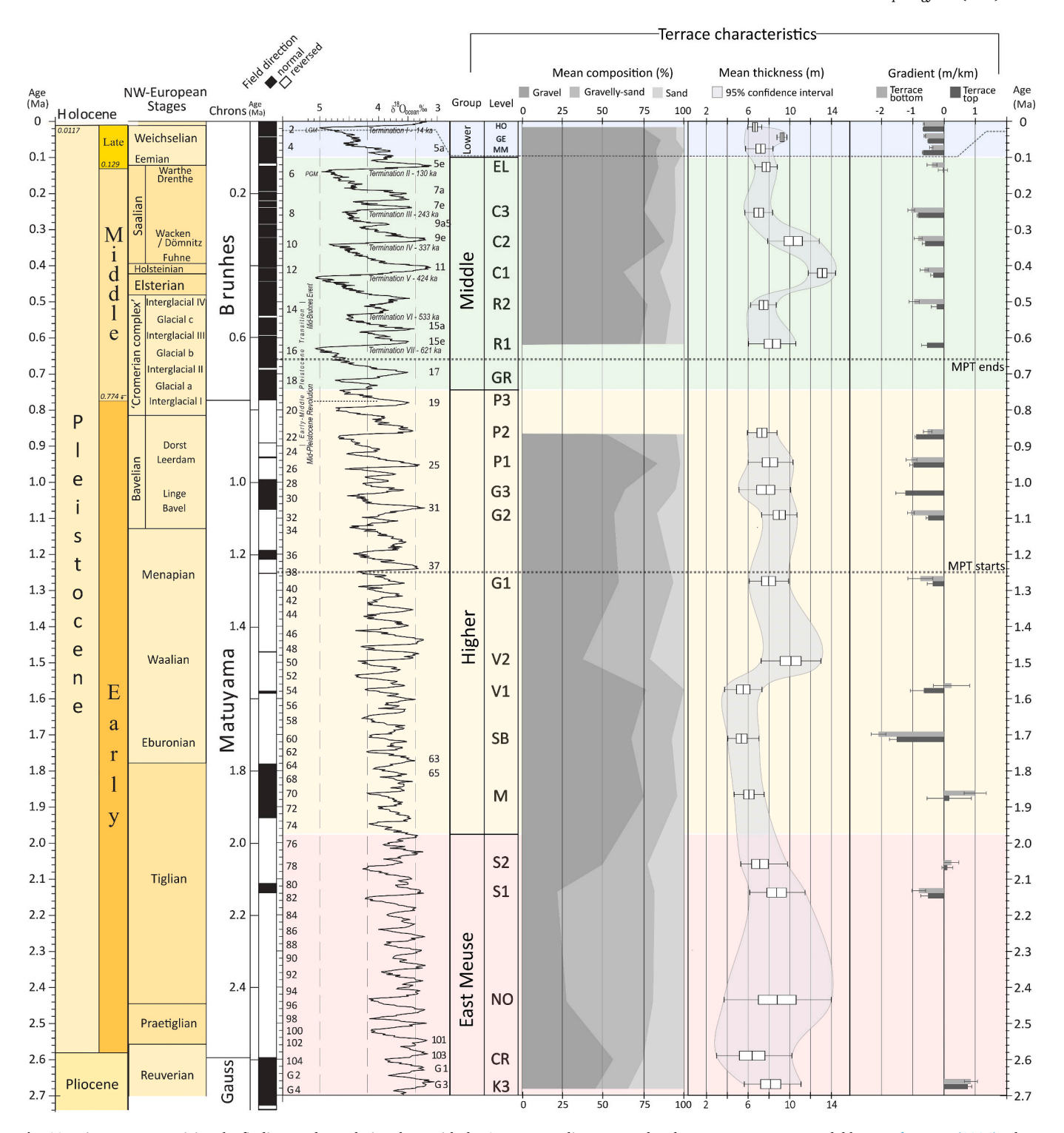


Fig. 10. Diagram summarizing the findings and correlating them with the Quaternary climate record and Meuse Terraces age model by Van den Berg (1996). Please note that the lines representing the start and end of the MPT are approximations, since these ages vary in the literature (see Clark et al., 2006); Chronostratigraphy after Cohen and Gibbard (2019); Oxygen isotope curve after Lisiecki and Raymo (2005); Terrace characteristics, this study. Levels Sint Pietersberg 3 (P3) and 's Gravenvoeren (GR) are not included due to lack of data. Gradients <0 km·m⁻¹ are dipping downstream, whereas gradients >0 m·km⁻¹ are reversed. The following terraces are not included in the gradient plot due to sparse data or implausible gradients: top terraces Noorbeek (NO) and Valkenburg (V2), and base terraces Crapoel (CR), Noorbeek (NO), Valkenburg 2 (V2), Sint Geertruid 3 (G3) and Rothem 1 (R1); Levels Crapoel (CR), Noorbeek (NO), and Valkenburg 2 (V2) are not included in the gradient plot due to extremely large uncertainties.

Meuse terrace record is not apparent. This can be attributed to its gradual nature, leading to a signal that might be dampened or assimilated by the broader signal generated by the overall changes in Quaternary climate. Another explanation could be related to the lag time

between the moment of a climatic/tectonic perturbation in the source and the formation of a terrace (e.g., Van Balen et al., 2010; Tofelde et al., 2019). However, the terraces are positioned immediately in front of the Ardennes. This fact combined with the gradually increasing, climate-

controlled transport capacity of the Meuse over the Quaternary indicates that the lag-time was probably short, so that a potential MPT signal should be effectively captured.

5.4. Gravel front migration

The gravel front in a fluvial system can be a reliable indicator of changes in boundary conditions (Allen, 2017), and its mobility is dependent on key factors such as local base level, degree of particle abrasion/break-down, sediment input, and river belt deposition width (i.e., Sambrook Smith and Ferguson, 1995; Murillo-Muñoz and Klaassen, 2006). The gravel content increase of the terrace record (Figs. 6 and 10) demonstrates how the Meuse gravel front gradually migrated downstream during the Quaternary. At the beginning of the Quaternary, the gravel front was most likely located south of Eijsden (location of the divergent point between East and West Meuse), since the East Meuse terraces are dominated by sand and gravelly sand (Fig. 10). Currently, the gravel front is located near the Peel Boundary Fault Zone at the northern limit of the Roer Valley Graben (about 80 km north of Maastricht; Murillo-Muñoz and Klaassen, 2006). The front migration can be explained by a combination of three factors: changing sediment source upstream, reworking of older terrace deposits and increasing incision and transport capacity of the river with time. Initially, the gravel was derived from the pre-Quaternary weathering mantle of the Ardennes. Subsequently, as incision into the bedrock ensued, the newly generated gravel gradually became coarser as a result of deeper incision into fresh or slightly weathered bedrock (see De Brue et al., 2015; Houbrechts et al., 2018).

The second factor is the reworking of older terrace deposits and selective transport of the fine-grained component during the incision and valley widening episode forming a new terrace level (Veldkamp and Van Dijke, 2000). The end-result of this process is a concentration of gravel, which is a mixture of gravel derived from older terraces and gravel freshly transported from upstream. This winnowing process during the formation of subsequent terrace levels results in a gradual rise in the proportion of gravel. It can be considered an autogenic process. In line with this, Van den Berg and Van Hoof (2001) suggested that the Meuse terraces deposits in the study area are part of an incised fan-like structure of which the apex migrated downstream during the Quaternary (see Fig. 2).

The third factor of gravel content increase is increasing transport capacity. Over the Quaternary, increased peak discharges can be attributed to longer and colder climatic conditions during the glacials (see Fig. 10). Seasonal snowmelt, frozen soils or permafrost, and sparse vegetation cover caused higher peak discharges during cold climatic conditions. This, in turn, led to a high transport capacity and the transportation of large amounts of gravel from the source area, accompanied by an increase in the general size of the transported gravel. In this line, modeling by Armitage et al. (2018) demonstrates that the gravel front responds well to cyclical changes in precipitation rates (and thus discharge and transport capacity). Despite significant lagged responses of the gravel front for longer periods of precipitation changes (over 200 ka), the response does not become buffered, demonstrating that the movement of the gravel front can be a reliable tool to diagnose climatic forcing (Armitage et al., 2018).

The increased river incision associated with the mid-Pleistocene uplift pulse in the Ardennes (around 0.78 Ma) is not evident in the gravel content increase, indicating that it did not significantly contribute to the migration of the gravel front by providing substantial amounts of gravel. A plausible explanation for this discrepancy could be the deceleration of upstream migration rates of knickpoints following this uplift episode (Rixhon et al., 2011; Sougnez and Vanacker, 2011; Rixhon and Demoulin, 2018).

6. Conclusions

This study demonstrates the response of the Meuse river to the Quaternary climatic changes and to an episode of increased tectonic uplift during the Mid-Pleistocene. The signals of such disturbances are (partially) preserved in the Meuse terrace deposits in front of the Ardennes (the source area) and are retrieved through systematic analysis of a large borehole database, supported by a detailed and updated terrace map.

Our analysis suggests that footwall back-tilting along the Feldbiss Fault Zone is reflected in the upstream dip of the East Meuse terraces, which likely had a low-gradient initially. The abandonment of the East Meuse valley in the late Tiglian is related to a combination of footwall back-tilting and increase of northward tectonic tilting, karstic processes, and capture by a local south-north drainage system.

Regarding the Quaternary climatic changes, our findings show that the increase in mean gravel content and weak increase in terrace thickness align with enhanced physical weathering and erosional processes in the Ardennes. This finding is corroborated by the low gravel content in the Early Pleistocene East Meuse terraces and relative high gravelly-sand and sand contents, which are explained by the erosion of the Neogene weathering mantle and sediments on the Ardennes. The increased gravel content of the West Meuse terraces is attributed to ongoing incision of the Meuse and erosion of fresh or partially weathered bedrock in the Ardennes, in combination with an enhanced transport capacity due to Pleistocene climate cooling and associated increase in the climate cycle amplitude. The gravel content analysis indicates a downstream migration of the Meuse gravel front during the Quaternary, driven by changes in the source upstream, local reworking and winnowing of older terrace deposits, and increasing transport capacity.

Surprisingly, the MPT, a gradual but major climatic transition, does not display a clear separate signal in the Meuse terrace record, although the gravel content does increase during the Quaternary. Enhanced valley incision, often proposed as an MPT response by other authors, did occur in the Meuse system, and is reflected by the transition from High to Middle terraces. However, the timing of this morphological transition shows that it can be linked to plume-induced uplift of the Ardennes, rather than the MPT.

Our findings are relevant to understanding the response of fluvial systems to the climate changes of the Quaternary, especially in NW Europe. However, the interpretation of our results is highly reliant on the age models proposed for these terraces, which bear significant uncertainties due to direct correlation of terrace levels to marine isotopic stages. Therefore, we suggest that more numerical ages for targeted terraces are key for unraveling the development of the Meuse terrace staircase and its response to environmental perturbations during the Quaternary. Also, future attempts to improve spatial correlation of terraces should consider their mineral content.

CRediT authorship contribution statement

Ewerton da Silva Guimarães: Writing – review & editing, Writing – original draft, Visualization, Validation, Software, Methodology, Investigation, Formal analysis, Data curation, Conceptualization. Freek S. Busschers: Writing – review & editing, Validation, Supervision, Software, Resources, Methodology, Investigation, Funding acquisition, Formal analysis, Data curation, Conceptualization. Cornelis Kasse: Writing – review & editing, Supervision, Methodology, Conceptualization. Tom Van Haren: Writing – review & editing, Resources. Armin Menkovic: Writing – review & editing, Resources. Ronald T. Van Balen: Writing – review & editing, Supervision, Resources, Project administration, Funding acquisition, Data curation, Conceptualization.

Declaration of competing interest

The authors declare that they have no known competing financial

interests or personal relationships that could have appeared to influence the work reported in this paper.

Data availability

Data will be made available on request.

Acknowledgements

This project has received funding from the European Union's Horizon 2020 research and innovation programme under the Marie Sklodowska-Curie grant agreement No 860383. The authors thank Ariel do Prado, Maxence Menthon, and Didier Roche for their support during the data processing stage. We also thank three anonymous reviewers for their comments and suggestions.

Appendix A. Supplementary data

Supplementary data to this article can be found online at https://doi.org/10.1016/j.geomorph.2024.109270.

References

- Allen, P.A., 2017. Dynamics of sediment routing systems. In: Sediment Routing Systems. Cambridge University Press, pp. 240–294. https://doi.org/10.1017/9781316135754.009
- Anderson, D.E., Goudie, A.S., Parker, A.G., 2013. Sea level changes of the Quaternary. In: Global Environments Through the Quaternary. Oxford University Press, pp. 197–228. https://doi.org/10.1093/acprof:osobl/9780199697267.003.0006.
- Armitage, J.J., Burgess, P.M., Hampson, G.J., Allen, P.A., 2018. Deciphering the origin of cyclical gravel front and shoreline progradation and retrogradation in the stratigraphic record. Basin Res. 30, 15–35. https://doi.org/10.1111/bre.12203.
- Beerten, K., Dreesen, R., Janssen, J., Van Uytven, D., 2018. The Campine Plateau. In: Demoulin, A. (Ed.), Landscapes and Landforms of Belgium and Luxembourg. Springer Science and Business Media B.V., pp. 193–214. https://doi.org/10.1007/ 978.3.310.582730.012
- Berends, C.J., Köhler, P., Lourens, L.J., van de Wal, R.S.W., 2021. On the cause of the Mid-Pleistocene transition. Rev. Geophys. 59 https://doi.org/10.1029/ 2020RG000727 e2020RG000727.
- Boenigk, W., 1978. Die flußgeschichtliche Entwicklung der Niederrheinischen Bucht im Jungtertiär und Altquartär. E&G Quat. Sci. J. 28, 1–9. https://doi.org/10.3285/EG 28 1 01
- Boenigk, W., Frechen, M., 2006. The Pliocene and Quaternary fluvial archives of the Rhine system. Quat. Sci. Rev. 25, 550–574. https://doi.org/10.1016/J. OUASCIREV.2005.01.018.
- Bosch, J.H.A., 2000. Standaard Boor Beschrijvingsmethode (NITG 00-141-A), 134 pp. Breuren, J.W.R., 1945. Het Terrassenlandschap van Zuid-Limburg. Med. Geol. Sticht. Ser. C VI, 93 pp.
- Bridgland, D., Westaway, R., 2008. Climatically controlled river terrace staircases: a worldwide Quaternary phenomenon. Geomorphology 98, 285–315. https://doi.org/ 10.1016/j.geomorph.2006.12.032.
- Bridgland, D.R., 1995. The Quaternary sequence of the eastern Thames basin: problems of correlation. In: Bridgland, D.R., Allen, P.A., Haggart, B.A. (Eds.), The Quaternary of Lower Reaches of the Thames. Quaternary Research Association, Durham, pp. 35–52
- Bridgland, D.R., 2006. The Middle and Upper Pleistocene sequence in the Lower Thames: a record of Milankovitch climatic fluctuation and early human occupation of southern Britain. Proc. Geol. Assoc. 117, 281–305. https://doi.org/10.1016/S0016-7878(06)80036-2.
- Bull, W., 1991. Geomorphic Responses to Climatic Change. Oxford University Press, Oxford, 326 pp.
- Bustamante-Santa Cruz, L., 1973. Heavy Minerals from Sandy Alluvium in the Meuse Basin. Katholieke Universiteit te Leuven, 355 pp.
- Clark, P.U., Pollard, D., 1998. Origin of the middle Pleistocene transition by ice sheet erosion of regolith. Paleoceanography 13, 1–9. https://doi.org/10.1029/ 97PA02660.
- Clark, P.U., Archer, D., Pollard, D., Blum, J.D., Rial, J.A., Brovkin, V., Mix, A.C., Pisias, N. G., Roy, M., 2006. The middle Pleistocene transition: characteristics, mechanisms, and implications for long-term changes in atmospheric pCO₂. Quat. Sci. Rev. 25, 3150–3184. https://doi.org/10.1016/j.quascirev.2006.07.008.
- Cohen, K.M., Gibbard, P.L., 2019. Global Chronostratigraphical Correlation Table for the Last 2.7 million years, Version 2019 QI-500. https://doi.org/10.1016/j. quaint.2019.03.009.
- Collard, S., Juvigné, E., Marion, J.-M., Mottequin, B., Petit, F., 2012. L'origine des mégalithes du Fond de Quarreux. Bull. Soc. Géogr. Liège 58, 33–51.
- Davison, A.C., Hinkley, D.V., 1997. Bootstrap Methods and Their Application, Bootstrap Methods and Their Application. Cambridge University Press. https://doi.org/ 10.1017/CBO9780511802843.

- De Brue, H., Poesen, J., Notebaert, B., 2015. What was the transport mode of large boulders in the Campine Plateau and the lower Meuse valley during the mid-Pleistocene? Geomorphology 228, 568–578. https://doi.org/10.1016/j. geomorph.2014.10.010.
- Demoulin, A., 1995. Les surfaces d'érosion méso-cénozoïques en Ardenne-Eifel. Bull. Soc. Géol. Fr. 573–585.
- Demoulin, A., Hallot, E., 2009. Shape and amount of the Quaternary uplift of the western Rhenish shield and the Ardennes (western Europe). Tectonophysics 474, 696–708. https://doi.org/10.1016/j.tecto.2009.05.015.
- Demoulin, A., Beckers, A., Rixhon, G., Braucher, R., Bourles, D., Siame, L., 2012. Valley downcutting in the Ardennes (W Europe): interplay between tectonically triggered regressive erosion and climatic cyclicity. Geol. Mijnbouw/Netherlands J. Geosci. 91, 79–90. https://doi.org/10.1017/s0016774600001517.
- Demoulin, A., Barbier, F., Dekoninck, A., Verhaert, M., Ruffet, G., Dupuis, C., Yans, J., 2018. Erosion surfaces in the Ardenne–Oesling and their associated kaolinic weathering mantle. In: Landscapes and Landforms of Belgium and Luxembourg. Springer Science and Business Media B.V., pp. 63–84. https://doi.org/10.1007/978-3-319-58239-9
- Ehlers, J., Gibbard, P.L., Hughes, P.D., 2018. Quaternary glaciations and chronology. In: Past Glacial Environments, Second ed., pp. 77–101. https://doi.org/10.1016/B978-0-08-100524-8 00003-8
- Felder, W.M., Bosch, P.W., 1989. Geologische kaart van Zuid-Limburg en omgeving. Afzettingen van de Maas.
- Fuller, T.K., Perg, L.A., Willenbring, J.K., Lepper, K., 2009. Field evidence for climatedriven changes in sediment supply leading to strath terrace formation. Geology 37, 467–470. https://doi.org/10.1130/G25487A.1.
- Geluk, M.C., Duin, E.J.T., Dusar, M., Rijkers, R.H.B., Van Den Berg, M.W., Van Rooijen, P., 1994. Stratigraphy and tectonics of the Roer Valley Graben. Geol. Mijnb. 73, 129-141
- Gibbard, P.L., Lewin, J., 2003. The history of the major rivers of southern Britain during the Tertiary. J. Geol. Soc. Lond. 160, 829–846. https://doi.org/10.1144/0016-764902-137.
- Gibbard, P.L., Lewin, J., 2009. River incision and terrace formation in the Late Cenozoic of Europe. Tectonophysics 474, 41–55. https://doi.org/10.1016/j. tecto.2008.11.017.
- Gildor, H., Tziperman, E., 2001. A sea ice climate switch mechanism for the 100-kyr glacial cycles. J. Geophys. Res. Oceans 106, 9117–9133. https://doi.org/10.1029/ 1999.IC000120.
- Gold, R.D., Friedrich, A., Kübler, S., Salamon, M., 2017. Apparent Late Quaternary faultslip rate increase in the southern Lower Rhine Graben, Central Europe. Bull. Seism. Soc. Am. 107, 563–580. https://doi.org/10.1785/0120160197.
- Gullentops, F., Bogemans, F., De Moor, G., Paulissen, E., Pissart, A., 2001. Quaternary lithostratigraphic units (Belgium). Geol. Belg. 4, 153–164. https://doi.org/ 10.20341/gb.2014.051.
- Head, M.J., Gibbard, P.L., 2015. Early-Middle Pleistocene transitions: linking terrestrial and marine realms. Quat. Int. 389, 7–46. doi:https://doi.org/10.1016/J.QUAINT.20 15.09.042.
- Helsel, D.R., Hirsch, R.M., Ryberg, K.R., Archfield, S.A., Gilroy, E.J., 2020. Statistical methods in water resources. In: U.S. Geological Survey Techniques and Methods, pp. 1–484. Book 4, chapter A3. B. 4, Hydrol. Anal. Interpret.
- Herbert, T.D., Peterson, L.C., Lawrence, K.T., Liu, Z., 2010. Tropical ocean temperatures over the past 3.5 million years. Science 328, 1530–1534. https://doi.org/10.1126/ SCIENCE 1185435
- Houbrechts, G., Petit, F., Van Campenhout, J., Juvigné, E., Demoulin, Alain, 2018. A unique boulder-bed reach of the Amblève River, Ardenne, at Fonds de Quarreux: modes of boulder transport. In: Demoulin, A. (Ed.), Landscapes and Landforms of Belgium and Luxembourg. Springer Science and Business Media B.V., pp. 85–99. https://doi.org/10.1007/978-3-319-58239-9
- Houtgast, R.F., Van Balen, R.T., 2000. Neotectonics of the Roer Valley Rift System, the Netherlands. Global Planet. Change 27, 131–146. https://doi.org/10.1016/S0921-8181(01)00063-7.
- Houtgast, R.F., Van Balen, R.T., Bouwer, L.M., Brand, G.B.M., Brijker, J.M., 2002. Late Quaternary activity of the Feldbiss Fault Zone, Roer Valley Rift System, the Netherlands, based on displaced fluvial terrace fragments. Tectonophysics 352, 295–315. https://doi.org/10.1016/S0040-1951(02)00219-6.
- Houtgast, R.F., Van Balen, R.T., Kasse, C., 2005. Late Quaternary evolution of the Feldbiss Fault (Roer Valley Rift System, the Netherlands) based on trenching, and its potential relation to glacial unloading. Quat. Sci. Rev. 24, 489–508. https://doi.org/10.1016/j.quascirev.2004.01.012.
- Huxtable, J., 1993. Further thermoluminescence dates for burnt flints from Maastricht-Belvédère and a finalized themolumiscence age for Unit IV Middle Palaeolithic sites. Meded. Rijks Geol. D 41–44.
- Juvigné, E., Renard, F., 1992. Les terrasses de la Meuse de Liège à Maastricht. Ann. Soc.
 Géol. Belg. 115, 167–186. https://popups.uliege.be/0037-9395.
 Kasse, C., 1988. Early Pleistocene Tidal and Fluviatile Environments in the Southern
- Kasse, C., 1988. Early Pleistocene Tidal and Fluviatile Environments in the Southern Netherlands and Northern Belgium. Ch. 6, PhD thesis.. Vrije Universiteit, Amsterdam.
- Kemna, H.A., 2008. A revised stratigraphy for the Pliocene and Lower Pleistocene deposits of the Lower Rhine embayment. Netherlands J. Geosci. 87, 91–105. https:// doi.org/10.1017/S0016774600024069.
- Kreemer, C., Blewitt, G., Davis, P.M., 2020. Geodetic evidence for a buoyant mantle plume beneath the Eifel volcanic area, NW Europe. Geophys. J. Int. 222, 1316–1332. https://doi.org/10.1093/GJI/GGAA227.
- Krook, L., 1993. Heavy minerals in the Belvédère deposits. Meded. Rijks Geol. D 47, 25–30.

Kuyl, O.S., 1980. Toelichtingen bij de geologische kaart van Nederland, 1:50 000, Blad Heerlen, 62W-62O. Rijks Geol. D. 1–206.

- Lawrence, K.T., Sosdian, S., White, H.E., Rosenthal, Y., 2010. North Atlantic climate evolution through the Plio-Pleistocene climate transitions. Earth Planet. Sci. Lett. 300, 329–342. https://doi.org/10.1016/J.EPSL.2010.10.013.
- Leeder, M.R., Gawthorpe, R.L., 1987. Sedimentary models for extensional tilt-block/half-graben basins. Geol. Soc. Lond. Spec. Publ. 28, 139–152. https://doi.org/10.1144/GSL.SP.1987.028.01.11.
- Lisiecki, L.E., Raymo, M.E., 2005. A Pliocene-Pleistocene stack of 57 globally distributed benthic $\delta^{18}O$ records. Paleoceanography 20, 1–17. https://doi.org/10.1029/2004PA001071.
- Lisiecki, L.E., Raymo, M.E., 2007. Plio-Pleistocene climate evolution: trends and transitions in glacial cycle dynamics. Quat. Sci. Rev. 26, 56–69. https://doi.org/ 10.1016/j.quascirev.2006.09.005.
- Losson, B., Quinif, Y., 2001. The Moselle piracy: new chronological data from U/Th dating of speleothems. Karstologia 29-40.
- Macar, P., 1938. Compte rendu de l'excursion du 24 avril 1938, consacrée à l'étude des terrasses de la Meuse entre Liége et l'Ubagsberg (Limbourg hollandais), pp. B187-B217.
- Macar, P., 1954. Les terraces fluviales et la Haute Belgique au Quaternaire. Prod. Une Descr. Géol. Belg. 18,, 591–606. https://popups.uliege.be/0037-9395/index.php? id=3396.
- Maddy, D., Bridgland, D., Westaway, R., 2001. Uplift-driven valley incision and climatecontrolled river terrace development in the Thames Valley, UK. Quat. Int. 79, 23–36. https://doi.org/10.1016/S1040-6182(00)00120-8.
- Maddy, D., Demir, T., Bridgland, D.R., Veldkamp, A., Stemerdink, C., van der Schriek, T., Schreve, D., 2007. The Pliocene initiation and Early Pleistocene volcanic disruption of the palaeo-Gediz fluvial system, Western Turkey. Quat. Sci. Rev. 26, 2864–2882. https://doi.org/10.1016/j.quascirev.2006.01.037.
- Martin, J.H., Gordon, R.M., Fitzwater, S.E., 1990. Iron in Antarctic waters. Nature 345, 156–158. https://doi.org/10.1038/345156a0.
- Martínez-García, A., Sigman, D.M., Ren, H., Anderson, R.F., Straub, M., Hodell, D.A., Jaccard, S.L., Eglinton, T.I., Haug, G.H., 2014. Iron fertilization of the subantarctic ocean during the last ice age. Science 343, 1347–1350. https://doi.org/10.1126/ science.1246848.
- Maslin, M.A., Ridgwell, A.J., 2005. Mid-Pleistocene revolution and the "eccentricity myth". Geol. Soc. Spec. Publ. 247, 19–34. https://doi.org/10.1144/GSL. SP.2005.247.01.02.
- Matoshko, A.V., Gozhik, P.F., Danukalova, G., 2004. Key Late Cenozoic fluvial archives of eastern Europe: the Dniester, Dnieper, Don and Volga. Proc. Geol. Assoc. 115, 141–173. https://doi.org/10.1016/S0016-7878(04)80024-5.
- McClymont, E.L., Sosdian, S.M., Rosell-Melé, A., Rosenthal, Y., 2013. Pleistocene seasurface temperature evolution: early cooling, delayed glacial intensification, and implications for the mid-Pleistocene climate transition. Earth Sci. Rev. 123, 173–193. https://doi.org/10.1016/J.EARSCIREV.2013.04.006.
- Meijer, T., Cleveringa, P., 2009. Aminostratigraphy of Middle and Late Pleistocene deposits in the Netherlands and the southern part of the North Sea Basin. Glob. Planet. Change 68, 326–345. https://doi.org/10.1016/j.gloplacha.2009.03.004.
- Meyer, W., Stets, J., 1998. Upper Pleistocene to recent tectonics in the Rhenish Massif and its quantitative analysis. Zeitsch. Dtsch. Geol. Gesellschaft 149, 359–379. https://doi.org/10.1127/zdgg/149/1998/359.
- Meyer, W., Stets, J., 2002. Pleistocene to recent tectonics in the Rhenish Massif (Germany). Netherlands J. Geosci. Geol. Mijnb. 81, 217–221. https://doi.org/ 10.1017/S0016774600022460.
- Michon, L., Van Balen, R.T., 2005. Characterization and quantification of active faulting in the Roer valley rift system based on high precision digital elevation models. Quat. Sci. Rev. 24, 455–472. https://doi.org/10.1016/j.quascirev.2003.11.009.
- Millero, F.J., 1995. Thermodynamics of the carbon dioxide system in the oceans. Geochim. Cosmochim. Acta 59, 661–677. https://doi.org/10.1016/0016-7037(94)
- Müller, J., Romero, O., Cowan, E.A., McClymont, E.L., Forwick, M., Asahi, H., März, C., Moy, C.M., Suto, I., Mix, A., Stoner, J., 2018. Cordilleran ice-sheet growth fueled primary productivity in the Gulf of Alaska, northeast Pacific Ocean. Geology 46, 307–310. https://doi.org/10.1130/G39904.1.
- Murillo-Muñoz, R., Klaassen, G., 2006. Downstream fining of sediments in the Meuse River. In: River Flow 2006. Taylor & Francis, pp. 895–905. https://doi.org/10.1201/ 9781439833865.ch94.
- Pazzaglia, F.J., 2013. 9.22 Fluvial terraces. In: Treatise on Geomorphology. Elsevier, pp. 379–412. https://doi.org/10.1016/B978-0-12-374739-6.00248-7.
- Pisias, N.G., Moore, T.C., 1981. The evolution of Pleistocene climate: a time series approach. Earth Planet. Sci. Lett. 52, 450–458. https://doi.org/10.1016/0012-821X (81)90197-7.
- Pissart, A., Harmand, D., Krook, L., 1997. The evolution of the Meuse from Toul to Maastricht from the Miocene to the present. Chronological correlations and age determinations of the captures of the lotharingian Meuse as reflected by the heavy minerals studies. Géog. Phys. Quatern. 51, 267–284. https://doi.org/10.7202/ 0221377AB
- Raymo, M.E., Lisiecki, L.E., Nisancioglu, K.H., 2006. Plio-pleistocene ice volume, antarctic climate, and the global δ^{18} O record. Science 313, 492–495. https://doi.org/10.1126/SCIENCE.1123296.
- Rea, B.R., Newton, A.M.W., Lamb, R.M., Harding, R., Bigg, G.R., Rose, P., Spagnolo, M., Huuse, M., Cater, J.M.L., Archer, S., Buckley, F., Halliyeva, M., Huuse, J., Cornwell, D.G., Brocklehurst, S.H., Howell, J.A., 2018. Extensive marine-terminating ice sheets in Europe from 2.5 million years ago. Sci. Adv. 4 https://doi.org/10.1126/ sci.adv.aar8327.

Rixhon, G., Demoulin, Alain, 2018. The picturesque Ardennian Valleys: Plio-Quaternary incision of the drainage system in the uplifting Ardenne. In: Demoulin, A. (Ed.), Landscapes and Landforms of Belgium and Luxembourg. Springer Science and Business Media B.V., pp. 159–175. https://doi.org/10.1007/978-3-319-58239-9_10

- Rixhon, G., Braucher, R., Bourlès, D., Siame, L., Bovy, B., Demoulin, A., 2011.

 Quaternary river incision in NE Ardennes (Belgium)—insights from ¹⁰Be/²⁶Al dating of river terraces. Quat. Geochronol. 6, 273–284. https://doi.org/10.1016/j. quageo.2010.11.001.
- Rixhon, G., Briant, R.M., Cordier, S., Duval, M., Jones, A., Scholz, D., 2017. Revealing the pace of river landscape evolution during the Quaternary: recent developments in numerical dating methods. Quat. Sci. Rev. 166, 91–113. https://doi.org/10.1016/j. quascirev.2016.08.016.
- Ruddiman, W.F., Raymo, M., Mcintyre, A., 1986. Matuyama 41,000-year cycles: North Atlantic Ocean and northern hemisphere ice sheets. Earth Planet. Sci. Lett. 80, 117, 120
- Sambrook Smith, G.H., Ferguson, R.I., 1995. The gravel-sand transition along river channels. SEPM J. Sediment. Res. 65A, 423–430. https://doi.org/10.1306/D42680E0-2B26-11D7-8648000102C1865D.
- Schaller, M., von Blanckenburg, F., Hovius, N., Veldkamp, A., van den Berg, M.W., Kubik, P.W., 2004. Paleoerosion rates from cosmogenic ¹⁰Be in a 1.3 Ma terrace sequence: response of the river Meuse to changes in climate and rock uplift. J. Geol. 112, 127–144. https://doi.org/10.1086/381654.
- Sosdian, S., Rosenthal, Y., 2009. Deep-sea temperature and ice volume changes across the Pliocene-Pleistocene climate transitions. Science 325, 306–310. https://doi.org/ 10.1126/science.1169938
- Sougnez, N., Vanacker, V., 2011. The topographic signature of Quaternary tectonic uplift in the Ardennes massif (Western Europe). Hydrol. Earth Syst. Sci. 15, 1095–1107. https://doi.org/10.5194/hess-15-1095-201.
- Spratt, R.M., Lisiecki, L.E., 2016. A Late Pleistocene sea level stack. Clim. Past 12, 1079–1092. https://doi.org/10.5194/cp-12-1079-2016.
- Su, Q., Wang, X., Gao, L., Yi, S., Han, Z., Ren, J., Vandenberghe, J., Lu, H., Van Balen, R., 2024. The impact of faulting-induced uplift and subsidence on terrace formation and abandonment: a case study of the Huangshui River, NE Tibetan Plateau. J. Geol. Soc. Lond. https://doi.org/10.1144/jgs2023-104.
- Tebbens, L.A., Veldkamp, A., Van Dijke, J.J., Schoorl, J.M., 2000. Modeling longitudinal-profile development in response to Late Quaternary tectonics, climate and sea-level changes: the River Meuse. Glob. Planet. Change 27, 165–186. https://doi.org/10.1016/S0921-8181(01)00065-0.
- Tesch, P., 1941. De schiervlakte van Eifel en Ardennen voor de opheffing tot Bergland. Geol. Mijnb. 273–277.
- Thompson, G.A., Parsons, T., 2016. Vertical deformation associated with normal fault systems evolved over coseismic, postseismic, and multiseismic periods. J. Geophys. Res. Solid Earth 121, 2153–2173. https://doi.org/10.1002/2015JB012240.
- Tofelde, S., Schildgen, T.F., Savi, S., Pingel, H., Wickert, A.D., Bookhagen, B., Wittmann, H., Alonso, R.N., Cottle, J., Strecker, M.R., 2017. 100 kyr fluvial cut-and-fill terrace cycles since the Middle Pleistocene in the southern Central Andes, NW Argentina. Earth Planet. Sci. Lett. 473, 141–153. https://doi.org/10.1016/J. EPSL.2017.06.001.
- Tofelde, S., Savi, S., Wickert, A.D., Bufe, A., Schildgen, T.F., 2019. Alluvial channel response to environmental perturbations: fill-terrace formation and sediment-signal disruption. Earth Surf. Dyn. 7, 609–631. https://doi.org/10.5194/esurf.7-609-2019.
- Tost, M., Cronin, S.J., Procter, J.N., Smith, I.E.M., Neall, V.E., Price, R.C., 2015. Impacts of catastrophic volcanic collapse on the erosion and morphology of a distal fluvial landscape: Hautapu River, Mount Ruapehu, New Zealand. Geol. Soc. Am. Bull. 127, 266–280. https://doi.org/10.1130/B31010.1.
- Tyráček, J., Westaway, R., Bridgland, D., 2004. River terraces of the Vltava and Labe (Elbe) system, Czech Republic, and their implications for the uplift history of the Bohemian Massif. Proc. Geol. Assoc. 115, 101–124. https://doi.org/10.1016/S0016-7878(04)80022-1.
- Van Balen, R.T., Houtgast, R.F., Van Der Wateren, F.M., Vandenberghe, J., Bogaart, P.W., 2000. Sediment budget and tectonic evolution of the Meuse catchment in the Ardennes and the Roer Valley Rift System. Glob. Planet. Change 27, 113–129. https://doi.org/10.1016/S0921-8181(01)00062-5.
- Van Balen, R.T., Houtgast, R.F., Cloetingh, S.A.P.L., 2005. Neotectonics of the Netherlands: a review. Quat. Sci. Rev. 24, 439–454. https://doi.org/10.1016/J. OUASCIREV.2004.01.011.
- Van Balen, R.T., Busschers, F.S., Tucker, G.E., 2010. Modeling the response of the Rhine–Meuse fluvial system to Late Pleistocene climate change. Geomorphology 114, 440–452. doi:https://doi.org/10.1016/j.geomorph.2009.08.007.
- Van Balen, R.T., Kasse, C., Wallinga, J., Woolderink, H.A.G., 2021. Middle to Late Pleistocene faulting history of the Heerlerheide fault, Roer Valley Rift System, influenced by glacio-isostasy and mining-induced displacement. Quat. Sci. Rev. 268, 107111 https://doi.org/10.1016/J.QUASCIREV.2021.107111.Van den Berg, M.W., 1989. Toelichting op kaartblad 59–62, geomorfologische kaart
- Van den Berg, M.W., 1989. Toelichting op kaartblad 59–62, geomorfologische kaart Nederland, 1:50.000. In: DLO-Staring Centrum. Wageningen/Rijks Geol. Dienst, Haarlem, 32 pp.
- Van den Berg, M.W., 1996. Fluvial Sequences of the Maas: A 10 Ma Record of Neotectonics and Climatic Change at Various Time-scales. PhD thesis.. University of Wageningen, Wageningen.
- Van den Berg, M.W., Van Hoof, T., 2001. The Maas terrace sequence at Maastricht, SE Netherlands: evidence for 200 m of late Neogene and Quaternary surface uplift. In: Maddy, D., Macklin, M.G., Woodward, J.C. (Eds.), River Basin Sediment Systems: Archives of Environmental Change. Balkema, Rotterdam, pp. 45–86.
- Van der Meulen, M.J., Doornenbal, J.C., Gunnink, J.L., Stafleu, J., Schokker, J., Vernes, R.W., van Geer, F.C., van Gessel, S.F., van Heteren, S., van Leeuwen, R.J.W., Bakker, M.A.J., Bogaard, P.J.F., Busschers, F.S., Griffioen, J., Gruijters, S.H.L.L.,

- Kiden, P., Schroot, B.M., Simmelink, H.J., van Berkel, W.O., van der Krogt, R.A.A., Westerhoff, W.E., van Daalen, T.M., 2013. 3D geology in a 2D country: perspectives for geological surveying in the Netherlands. Netherlands. J. Geosci. Geol. Mijnb. 92, 217–241. https://doi.org/10.1017/S0016774600000184.
- Van Haren, T., Dirix, K., De Koninck, R., De Groot, C., De Nil, K., 2016a. An interactive voxel model for mineral resources: loess deposits in Flanders (Belgium). Zeitschrift Dtsch. Gesellschaft Geowissenschaften 167, 363–376. https://doi.org/10.1127/ zdeg/2016/0096.
- Van Haren, T., Dirix, K., De Koninck, R., 2016b. Thematisch delfstoffenmodel Zanden grindafzettingen van Maas en Rijn in Vlaanderen. In: VITO NV. ETE/1310192-01/2016-0001.
- Van Kolfschoten, T., Roebroeks, W., Vandenberghe, J., 1993. The middle and late Pleistocene climatic sequence at Maastricht-Belvedere: the type locality of the Belvedere interglacial. Meded. Rijks Geol. D 47, 81–91.
- Van Straaten, L.M.J.U., 1946. Grindonderzoek in Zuid-Limburg. In: Meded. Geol. Stichting Serie C-VI-2.
- Vandenberghe, J., 2008. The fluvial cycle at cold–warm–cold transitions in lowland regions: a refinement of theory. Geomorphology 98, 275–284. https://doi.org/ 10.1016/J.GEOMORPH.2006.12.030.
- Vandenberghe, J., 2015. River terraces as a response to climatic forcing: formation processes, sedimentary characteristics and sites for human occupation. Quat. Int. 370, 3–11. https://doi.org/10.1016/J.QUAINT.2014.05.046.
- Vandermaelen, N., Vanacker, V., Clapuyt, F., Christl, M., Beerten, K., 2022. Reconstructing the depositional history of Pleistocene fluvial deposits based on grain size, elemental geochemistry and in-situ ¹⁰Be data. Geomorphology 402, 108127. https://doi.org/10.1016/J.GEOMORPH.2022.108127.
- Veldkamp, A., Van Dijke, J.J., 2000. Simulating internal and external controls on fluvial terrace stratigraphy: a qualitative comparison with the Maas record. Geomorph 33, 225–236. https://doi.org/10.1016/S0169-555X(99)00125-7.
- Westaway, R., 2001. Flow in the lower continental crust as a mechanism for the Quaternary uplift of the Rhenish Massif, northwest Europe. In: Maddy, D.,

- Macklin, M.G., Woodward, J.C. (Eds.), River Basin Sediment Systems: Archives of Environmental Change. Balkema, pp. 87–167.
- Westerhoff, W.E., Kemna, H.A., Boenigk, W., 2008. The confluence area of Rhine, Meuse, and Belgian rivers: Late Pliocene and Early Pleistocene fluvial history of the northern Lower Rhine Embayment. Netherlands. J. Geosci. Geol. Mijnb. 87, 107–125. https://doi.org/10.1017/S0016774600024070.
- Woolderink, H.A.G., Kasse, C., Cohen, K.M., Hoek, W.Z., Van Balen, R.T., 2019. Spatial and temporal variations in river terrace formation, preservation, and morphology in the Lower Meuse Valley, The Netherlands. Quatern. Res. 91, 548–569. https://doi.org/10.1017/qua.2018.49.
- Yehudai, M., Kim, J., Pena, L.D., Jaume-Seguí, M., Knudson, K.P., Bolge, L., Malinverno, A., Bickert, T., Goldstein, S.L., 2021. Evidence for a Northern Hemispheric trigger of the 100,000-y glacial cyclicity. Proc. Natl. Acad. Sci. 118 https://doi.org/10.1073/PNAS.2020260118 e2020260118.
- Yuan, X.P., Guerit, L., Braun, J., Rouby, D., Shobe, C.M., 2022. Thickness of fluvial deposits records climate oscillations. J. Geophys. Res. Solid Earth 127. https://doi. org/10.1029/2021JB023510 e2021JB023510.
- Zachos, J., Pagani, H., Sloan, L., Thomas, E., Billups, K., 2001. Trends, rhythms, and aberrations in global climate 65 Ma to present. Science 292, 686–693. https://doi. org/10.1126/science.1059412.
- Zagwijn, W.H., 1985. An outline of the Quaternary stratigraphy of the Netherlands. Geol. Mijnb. 64, 17–24.
- Ziegler, P.A., 1992. European Cenozoic rift system. Tectonophysics 208, 91–111. https://doi.org/10.1016/0040-1951(92)90338-7.
- Ziegler, P.A., Dèzes, P., 2007. Cenozoic Uplift of Variscan Massifs in the Alpine Foreland: Timing and Controlling Mechanisms. https://doi.org/10.1016/j. gloplacha.2006.12.004.
- Zonneveld, J.I.S., 1949. Zand-petrologische onderzoekingen in de terrassen van Zuid-Limburg. Med. Geol. Sticht. Ser. 3, 103–123.